Texas Tech University

Multidisciplinary Research in Transportation

Pilot Implementation of Whitetopping: Final Report

Wujun Zhou, Pangil Choi, Sungwoo Ryu, and Moon C. Won

Performed in cooperation with the Texas Department of Transportation

and the Federal Highway Administration

Research Project 5-5482-01

Research Report 5-5482-01-1

http://www.techmrt.ttu.edu/reports.php

Technical Report Documentation Page

1. Report No. FHWA/TX-17/5-5482-01-1	2. Government Accession No.	3. Recipient's Catalog No.
4. Title and Subtitle Pilot Implementation of Whitetopping: Final Report		5. Report Date August 2013; Published December 2017
		6. Performing Organization Code
7. Author(s) Wujun Zhou, Pangil Choi, Sungwoo Ryu, Moon C. Won		8. Performing Organization Report No. 5-5482-01-1
9. Performing Organization Name and Address Texas Tech University College of Engineering Box 41023 Lubbock, Texas 79409-1023		10. Work Unit No. (TRAIS)
		11. Contract or Grant No. 5-5482-01
12. Sponsoring Agency Name and Address Texas Department of Transportation Research and Technology Implementation Division P.O. Box 5080 Austin, TX 78763-5080		13. Type of Report and Period Covered Technical Report 09/2010-08/2013
		14. Sponsoring Agency Code

15. Supplementary Notes
Project performed in cooperation with the Texas Department of Transportation and the Federal Highway Administration.

16. Abstract
The design of whitetopping has been based on experience. The current TxDOT whitetopping design is based on American Concrete Pavement Association (ACPA), which does not consider the condition of existing asphalt pavement. Recognizing the limitations of this procedure, TxDOT sponsored a research study to develop mechanistic-empirical pavement design for whitetopping under the TxDOT Research Project 0-5482. Two whitetopping projects were constructed and their mechanistic behavior and early-age performance have been evaluated, with the primary objective being to validate the design procedure developed in 0-5482. However, the whitetopping projects are less than 2 years old, and the validation of the procedure for long-term performance could not be made. However, performance evaluations of a number of whitetopping projects built under old designs have provided valuable information and design guidelines were developed.

The performance of the two projects with 6-ft by 6-ft joint spacing needs to be monitored for the differential slab movements potential at longitudinal joints to determine whether tie bars are necessary or not. Until more conclusive findings are made, it is recommended that tie bars are not used in whitetopping.

All the whitetopping projects in Texas, except for the section in Loy Lake Drive, did not have joints sealed. No adverse effects of not sealing the joints have been observed in whitetopping projects in Texas. The performance of the Emory project needs to be monitored for the evaluations of joints with no seals in high rainfall areas. At this point, national efforts are underway by 'Seal or Not Seal (SNS) Group' to positively determine whether sealing is really needed for joints in CPCD or whitetopping. Until SNS suggests conclusive findings and recommendations, it is recommended that joints in the whitetopping are not sealed.

17. Key Words Whitetopping, mechanistic-empirical pavement design, saw cut design		18. Distribution Statement No restrictions. This document is available to the public through the National Technical Information Service, Springfield, Virginia 22161; www.ntis.gov.	
19. Security Classif. (of report) Unclassified	20. Security Classif. (of this page) Unclassified	21. No. of pages 62	22. Price

Form DOT F 1700.7 (8-72) Reproduction of completed page authorized

Pilot Implementation of Whitetopping: Final Report

Wujun Zhou, Ph.D.
Post-Doctoral Fellow of Civil and Environmental Engineering
Texas Tech University

Pangil Choi, Ph.D.
Post-Doctoral Fellow of Civil and Environmental Engineering
Texas Tech University

Sungwoo Ryu, Ph.D.
Post-Doctoral Fellow of Civil and Environmental Engineering
Texas Tech University

Moon C. Won, Ph.D., P.E.
Professor of Civil, Environmental, and Construction Engineering
Texas Tech University

Research Report Number 5-5482-01-1
Project Number 5-5482

Conducted for the Texas Department of Transportation

Center for Multidisciplinary Research in Transportation
Texas Tech University

AUTHOR'S DISCLAIMER

The contents of this report reflect the views of the authors who are responsible for the facts and the accuracy of the data presented herein. The contents do not necessarily reflect the official view of policies of the Texas Department of Transportation or the Federal Highway Administration. This report does not constitute a standard, specification, or regulation.

PATENT DISCLAIMER

There was no invention or discovery conceived or first actually reduced to practice in the course of or under this contract, including any art, method, process, machine, manufacture, design or composition of matter, or any new useful improvement thereof, or any variety of plant which is or may be patentable under the patent laws of the United States of America or any foreign country.

ENGINEERING DISCLAIMER

Not intended for construction, bidding, or permit purposes.

TRADE NAMES AND MANUFACTURERS' NAMES

The United States Government and the State of Texas do not endorse products or manufacturers. Trade or manufacturers' names appear herein solely because they are considered essential to the object of this report.

ACKNOWLEDGMENTS

This research study was sponsored by the Texas Department of Transportation in cooperation with the Federal Highway Administration. The authors express their gratitude to Dr. Dar Hao Chen, project director, PMC members, and RTI Program Manager, Mr. Darrin Jensen. In addition, the authors acknowledge the support provided by the Paris District personnel during the construction of whitetopping sections.

Table of Contents

List of Figures

List of Tables

Chapter 1 Introduction

Asphalt pavements with severe distresses provide excellent candidates for Portland cement concrete (PCC) overlay (called whitetopping), especially in intersection areas. Two intersections in the Paris District with asphalt pavement experienced rutting distress and were ideal candidates for whitetopping, since repeated asphalt overlays did not mitigate the long-term rutting distress.

The design of whitetopping has been based on experience. The current TxDOT whitetopping design is based on the American Concrete Pavement Association (ACPA), which does not consider the condition of existing asphalt pavement (TxDOT 2011). Recognizing the limitations of this procedure, TxDOT sponsored a research study to develop mechanistic-empirical pavement design for whitetopping.

In TxDOT research project 0-5482, mechanistic-empirical whitetopping design procedure was developed, which considered the support condition in the existing asphalt pavement (Kim et al. 2008; Suh et al. 2008). In this implementation project, the newly developed whitetopping design procedure was applied to develop optimum designs. It is expected that the whitetopping pavement system at the two locations that will be designed by the new design procedure will provide long-lasting pavement system with satisfactory performance.

The primary objective of this implementation project was to develop whitetopping designs for the two locations in the Paris District and to provide technical support during the PS&E preparation and construction stages. The research team worked closely with the implementation director and district staff to facilitate the implementation of whitetopping for the two locations in the Paris District. For these two locations, the slab thickness, joint details and transition section designs were developed and provided for the preparation of PS&E and implementation.

Chapter 2 Construction of Whitetopping Sections

Whitetopping sections were constructed in two locations in the Paris District with the designs developed from the new mechanistic-empirical design procedure developed under the TxDOT Research Project 0-5482, and their early-age behavior and performance were evaluated. Because the new design procedure requires the conditions of supporting layers as input variables, the properties of supporting layers were evaluated by falling weight deflectometer (FWD), coring, and dynamic cone penetrometer (DCP) testing. Once the properties of supporting layers, such as modulus of subgrade reaction (k) and modulus values of each layer, were estimated, those values were used as inputs for whitetopping thickness design.

2.1 Loy Lake Project

The Loy Lake section is located at the intersection of Loy Lake Road and US 75 North Frontage Road as indicated in Figure 2.1. The asphalt concrete pavement (ACP) in this section was a good candidate for whitetopping construction as the ACP underwent a number of rutting and shoving distresses with a potential hydroplaning problem. With the input values thus obtained, along with design traffic, whitetopping design thickness was determined from the afore-mentioned mechanistic-empirical design procedure

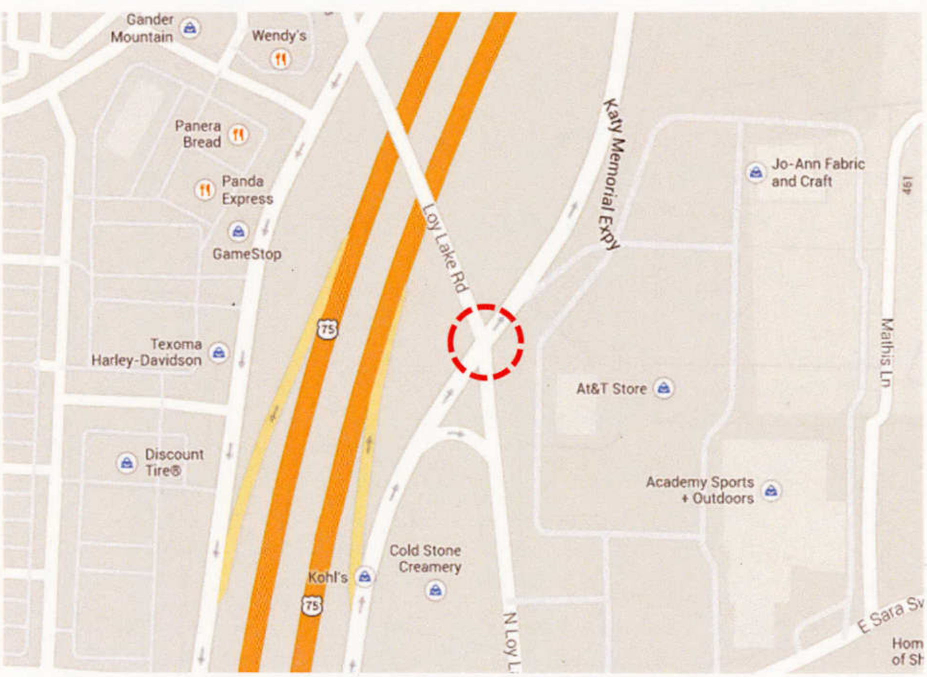

Figure 2.1 Location of Loy Lake section

2.1.1 Thickness Design

The thickness design equation in the mechanistic-empirical design procedure developed under 0-5482 for whitetopping pavement is as follows (Suh et al. 2008):

$$\begin{aligned}\text{Log}\,(t_{PCC}) = {} & 3.5615 + 0.1017\cdot\log(ESALs) + 0.4982\cdot\log(E_{PCC}) - 0.7232\cdot\log(t_{AC}) \\ & - 0.3624\cdot\log(E_{AC}) - 0.2695\cdot\log(t_{BS}) - 0.0891\cdot\log(E_{BS}) - 0.0287\cdot\log(k) \\ & - 1.2250\cdot\log(MR)\end{aligned}$$

<Eq.1>

where,

t_{PCC} = required thickness of the whitetopping concrete, in,
ESALs = expected number of 18-kips ESALs,
E_{PCC} = concrete modulus of elasticity, psi,
t_{AC} = thickness of the asphalt layer, in,
E_{AC} = asphalt modulus of elasticity, psi,
t_{BS} = thickness of the base layer, in,
E_{BS} = base modulus of elasticity, psi,
k = modulus of subgrade reaction, pci, and
MR = modulus of rupture of whitetopping concrete, psi.

The above equation was used to determine the design thickness for the whitetopping section.

2.1.1.1 Coring and GPR

FWD and DCP tests as well as coring were conducted at the designated locations by TxDOT personnel indicated in Figure 2.1. Given the data obtained from four core samples, the section was divided into three areas as shown in Figure 2.2. The thickness of existing asphalt concrete pavement (ACP) was evaluated using a ground-penetrating radar (GPR). The GPR was operated by the TxDOT. Figure 2.3 presents the ACP thicknesses estimated by GPR on the basis of total five runs. The result showed that the existing ACP thickness had a large variation from 2 to 13 in.

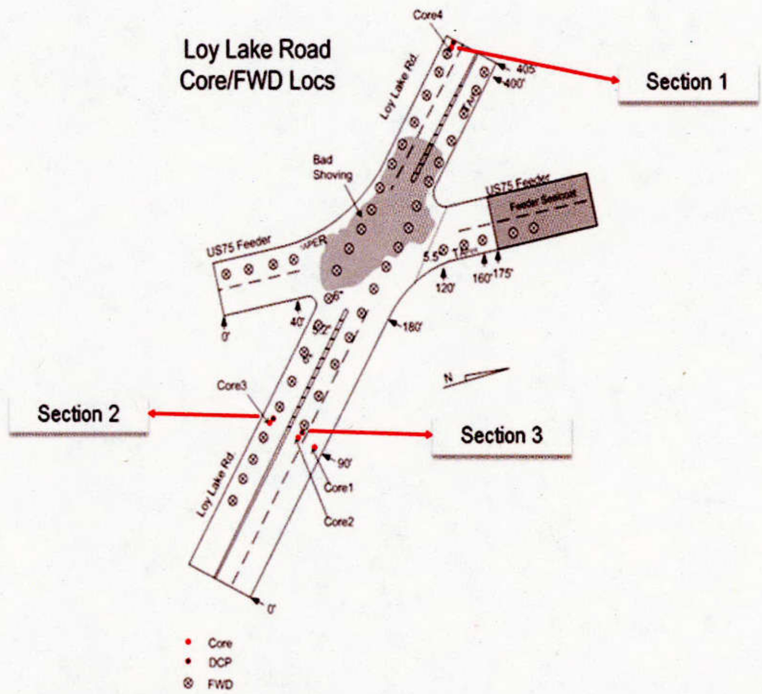

Figure 2.2 Location for Coring and FWD

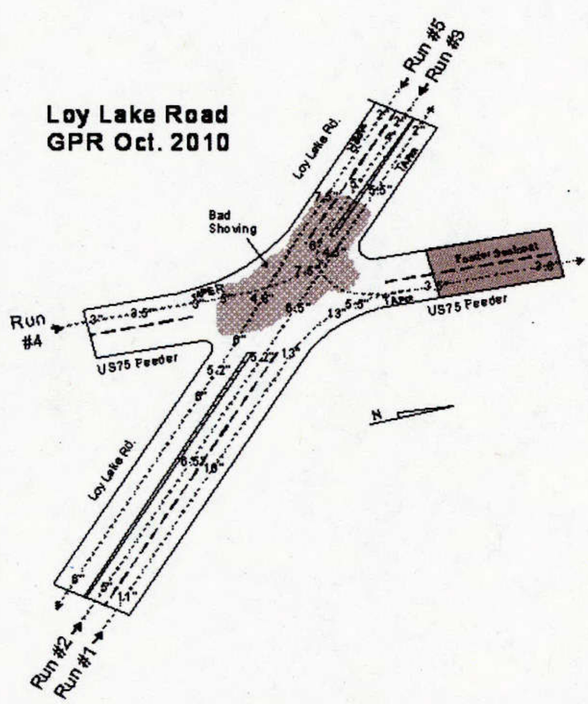

Figure 2.3 Existing Asphalt Thickness (Loy Lake Road)

2.1.1.2 FWD and Traffic Analysis

Table 2.1 presents the FWD data obtained from the TxDOT. Also, Figure 2.4 shows the daily traffic data recorded for various directions. Based on the given traffic data, ESALs were estimated using Eq. 2 with 10 and 20 years design lives for four different directions. The traffic data and design ESAL for each of the directions are summarized in Table 2.2.

$$\text{ESALs} = (\text{trucks per day}) \times 2 \times 365 \times (\text{design life in years}) \qquad \text{<Eq. 2>}$$

Table 2.1 FWD Data of Section 1 to 3

Location	Load Level (lbs)	Deflection (mils)						
		Geophone distance from the loading plate (inch)						
		0	12	24	36	48	60	72
Section 1	9173	22.3	13.03	5.69	2.82	1.65	1.31	1.2
Section 2	9355	16.26	8.58	3.85	2.5	1.81	1.69	1.22
Section 3	9451	11.54	6.59	3.19	1.89	1.26	1.16	0.91
Section 1	Equalized to 9000lbs.	21.9	12.8	5.6	2.8	1.6	1.3	1.2
Section 2		15.6	8.3	3.7	2.4	1.7	1.6	1.2
Section 3		11.0	6.3	3.0	1.8	1.2	1.1	0.9

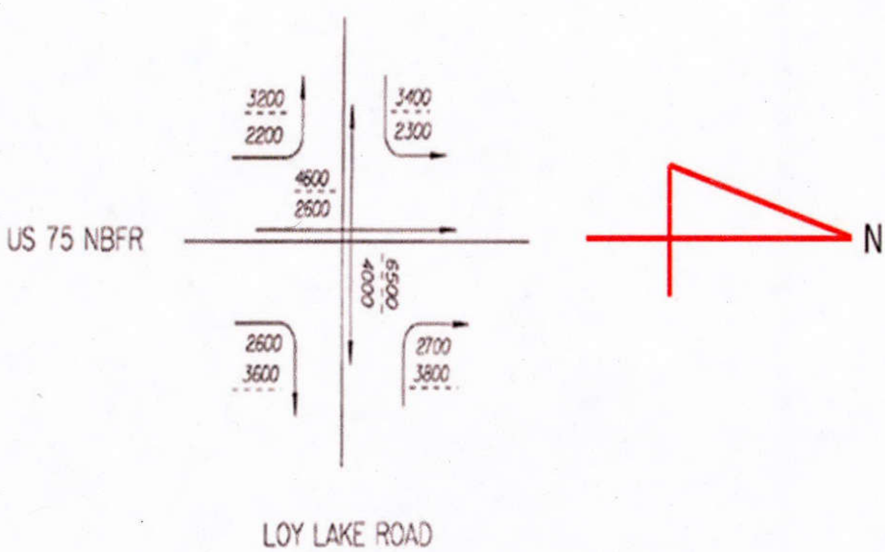

Figure 2.4 Traffic Data and Direction

Table 2.2 Traffic Data and Design ESAL for Each Direction

	Design Year	*Direction 1*	*Direction 2*	*Direction 3*	*Total ADT*	*# Truck (18.4 %)*	*ESALs*
South	2010	2200	2600	2600	7400	1,362	993,968
	2020				9400	1,730	12,626,080
	2030	3200	4600	3600	11400	2,098	30,624,960
North	2010	2300	2600	2700	7600	1,398	1,020,832
	2020				10650	1,960	14,305,080
	2030	3400	3800	6500	13700	2,521	36,803,680
East	2010	2700	4000	2600	9300	1,711	1,249,176
	2020				11600	2,134	15,581,120
	2030	3800	6500	3600	13900	2,558	37,340,960
West	2010	2300	4000	2200	8500	1,564	1,141,720
	2020				10800	1,987	14,506,560
	2030	3400	6500	3200	13100	2,410	35,191,840

2.1.1.3 DCP

The correlation between the number of blows and corresponding penetration depths was assessed for the DCP data. DCP data was converted to CBR values using Eq. 3. The slope input in Eq. 3 could be obtained from the result of DCP tests. Once CBR values were obtained, the moduli of subbase or subgrade were evaluated using Eq. 4 (TxDOT 2011). The results of DCP tests and corresponding CBR and moduli evaluated for all three subsections are presented in Table 2.3.

$$\text{CBR} = 292/\text{Slope of DCP plot (mm/blow)}^2 \qquad \text{<Eq. 3>}$$

$$\text{Modulus (ksi)} = 2.55 * \text{CBR}^{0.64} \qquad \text{<Eq. 4>}$$

Table 2.3 Modulus and CBR value for each section

		Section 1	Section 2	Section 3
Layer 1	mm/blow	0.701	0.497	0.555
	CBR	434.55	639.67	564.19
	Modulus	124.42	159.35	147.05
Layer 2	mm/blow	1.071		
	CBR	270.29		
	Modulus	91.82		

2.1.1.4 Thickness Design

As can be seen in Equation 1, ACP thickness is an input for the whitetopping design. The thickness of ACP was measured from both core sample and GPR. Three different asphalt concrete thicknesses obtained from three areas were chosen to calculate whitetopping design thicknesses. The MR and E_{PCC} were assumed to be 620 psi 4,000,000 psi, respectively. A summary of inputs used for the design of whitetopping is presented in Table 2.4.

Table 2.4 Input for Whitetopping Thickness

	Section 1		Section 2		Section 3	
	10 years	20 years	10 years	20 years	10 years	20 years
$ESALs$ (x10^6)	14.5	35.2	15.6	37.3	15.6	37.3
E_{PCC} (psi)	4,000,000	4,000,000	4,000,000	4,000,000	4,000,000	4,000,000
t_{AC} (inch)	2.75	2.75	6.00	6.00	5.75	5.75
t_{BS} (inch)	12.25	12.25	8.00	8.00	8.25	8.25
E_{BS} (psi)	108.25	108.25	159.35	159.35	147.05	147.05
k (psi/inch)	305	305	456	456	589	589
MR (psi)	620	620	620	620	620	620

Table 2.5 shows the final whitetopping design thickenesses for various design lives and E_{AC}, evaluated based on the inputs provided in Table 2.4. Because exact values of E_{AC} could not be obtained, design thicknesses were calculated for a wide range of E_{AC}, from 500,000 to 2,000,000 psi. It shows that Section 1 has the lowest slab support condition and requires the largest slab thickness. Based on this analysis, a design thickness of 6 in was selected for the project.

Table 2.5 Whitetopping Thickness

		Whitetopping Thickness					
		Sec.1		Sec.2		Sec.3	
		10 yr	20 yr	10 yr	20 yr	10 yr	20 yr
E_{AC} (psi)	500,000	9.4	*10.3*	5.6	6.1	5.8	6.3
	750,000	8.1	*8.9*	4.9	5.3	5.0	5.4
	1,000,000	7.3	*8.0*	4.4	4.8	4.5	4.9
	1,250,000	6.7	*7.4*	4.0	4.4	4.1	4.5
	1,500,000	6.3	*6.9*	3.8	4.1	3.9	4.2
	1,750,000	6.0	*6.5*	3.6	3.9	3.7	4.0
	2,000,000	5.7	*6.2*	3.4	3.7	3.5	3.8

2.1.2 Saw Cut Design

Based on the final whitetopping design thickness of 6 in., the section design for Loy Lake Road and US 75 Frontage Road section was devised. The dimensions of a saw cut panel were 6 ft. by 6 ft. Figure 2.5 depicts the section information including the saw cut design. As the figure shows, the length of Loy Lake Road (STA. 4+20.00 to STA. 8+20.00) was 400 ft, and the length of Frontage Road (STA. 1067+79.89 to STA. 1068+79.89) was 100 ft.

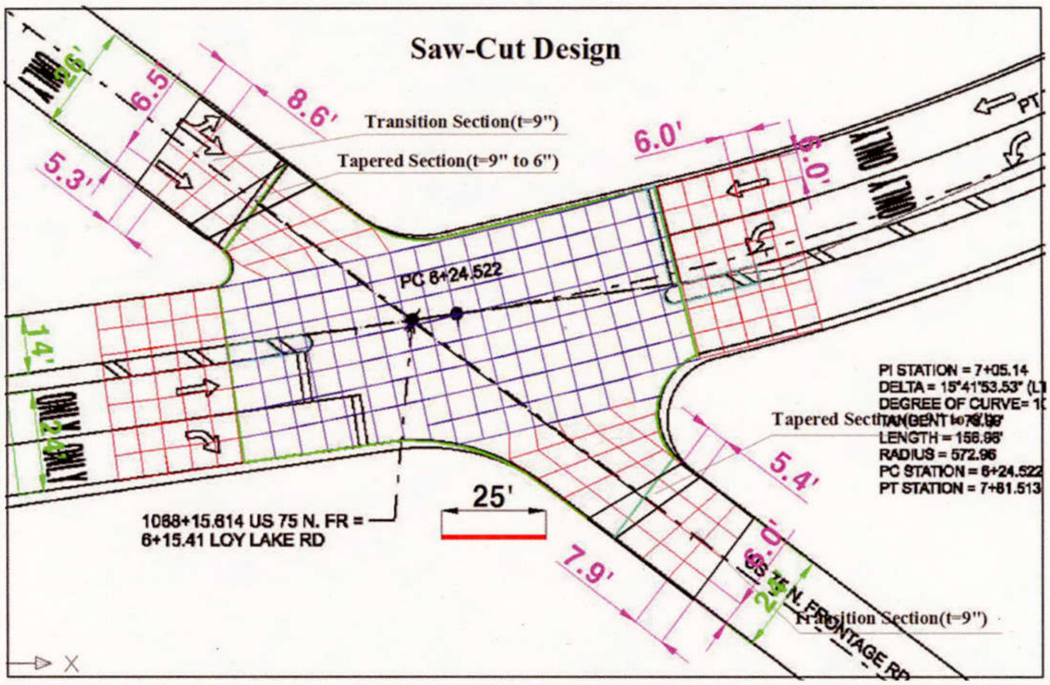

Figure 2.5 Plan View of the Design Section

2.1.3 Design of Transection Section

Figure 2.6 shows the plan view and corresponding elevation profile of Loy Lake Road. West end of the whitetopping section on Loy Lake abuts bridge approach slab. The elevation of bridge approach slab was slightly higher than that of whitetopping section as can be seen in Figure 2.6. Since it was expected that the behavior between the bridge approach slab and whitetopping is significantly different, a special design for transition section was developed to minimize the potential for distresses at the joint area between whitetopping and bridge approach slab. Figures 2.7 and 2.8 illustrate the plan view and cross-sectional design of transition area, respectively. Steel reinforcement such as CRCP was designed to provide the continuity within the whitetopping slabs near the bridge approach slab. Saw cuts were also designed to relieve concrete stresses from environmental loading (temperaure and moisture variations) as shown in Figure 2.7. As can be seen in Figure 2.8, dowel bars were installed to provide a sufficient level of load transfer efficiency (LTE) between the bridge approach slab and whitetopping section.

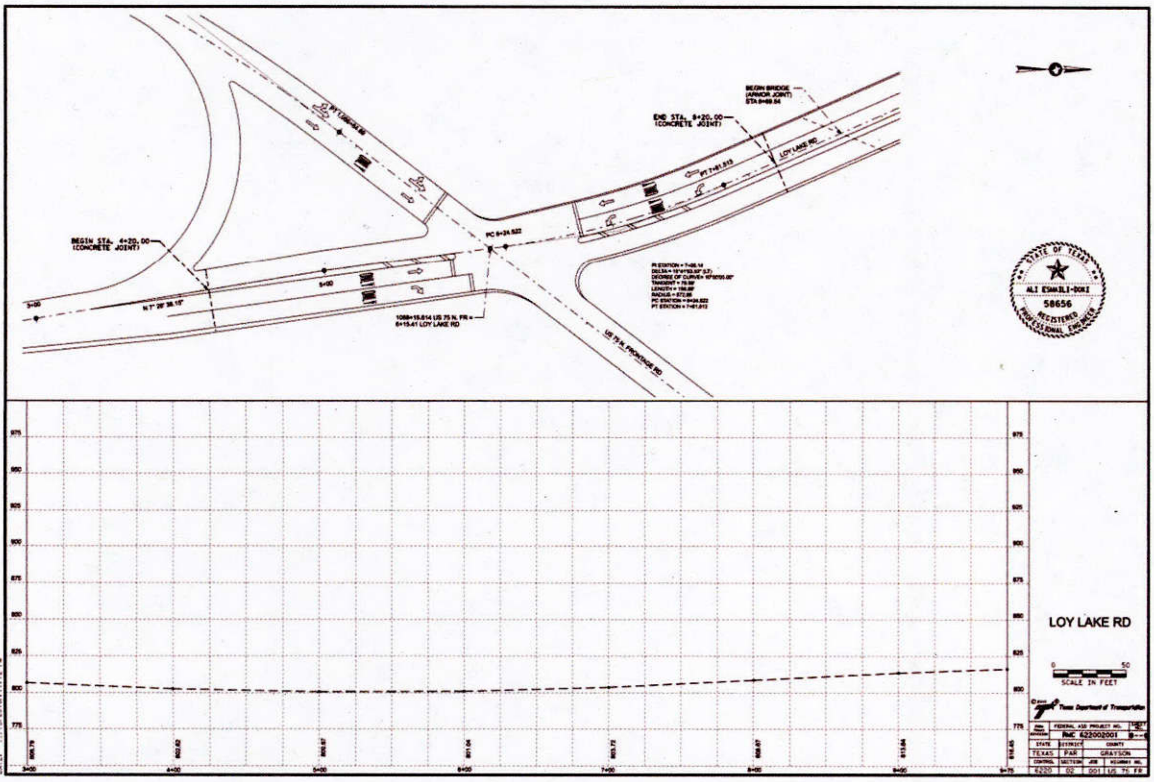

Figure 2.6 Plan View and Elevation of Loy Lake Rd

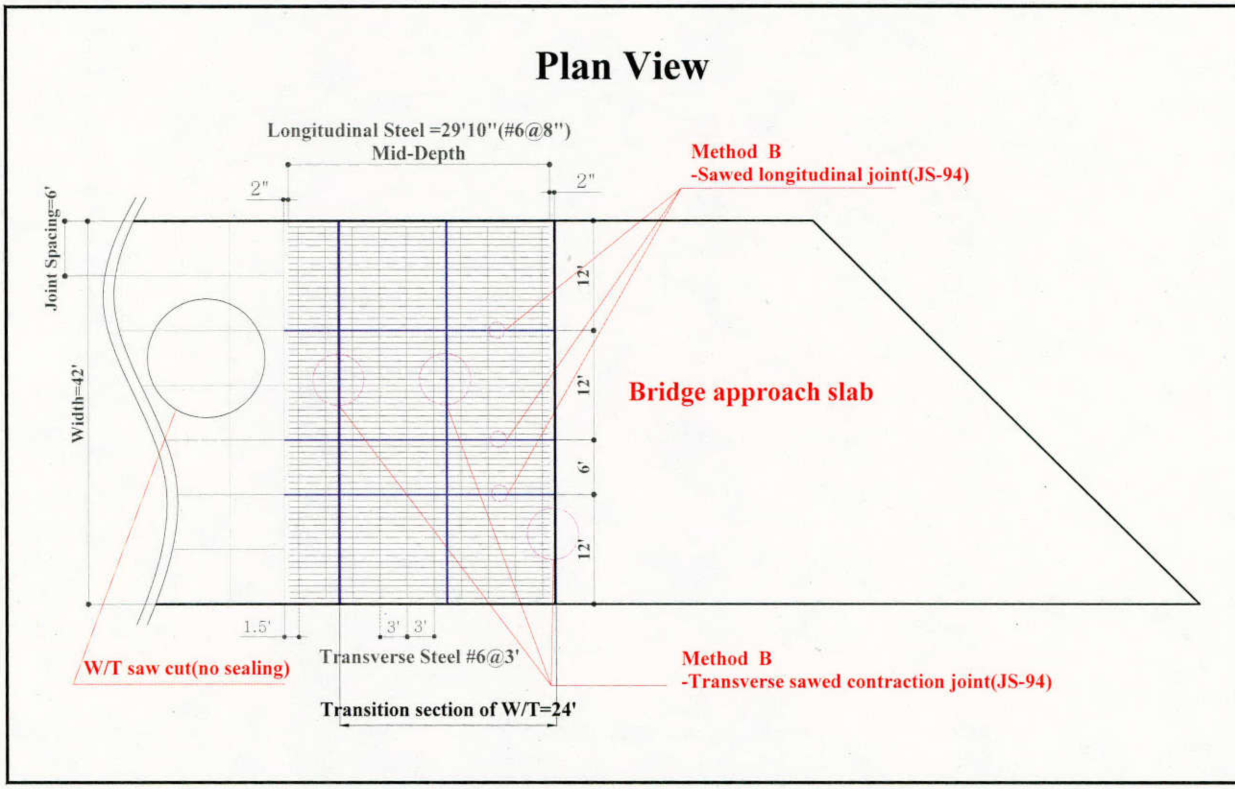

Figure 2.7 Transition Section Design (plan view)

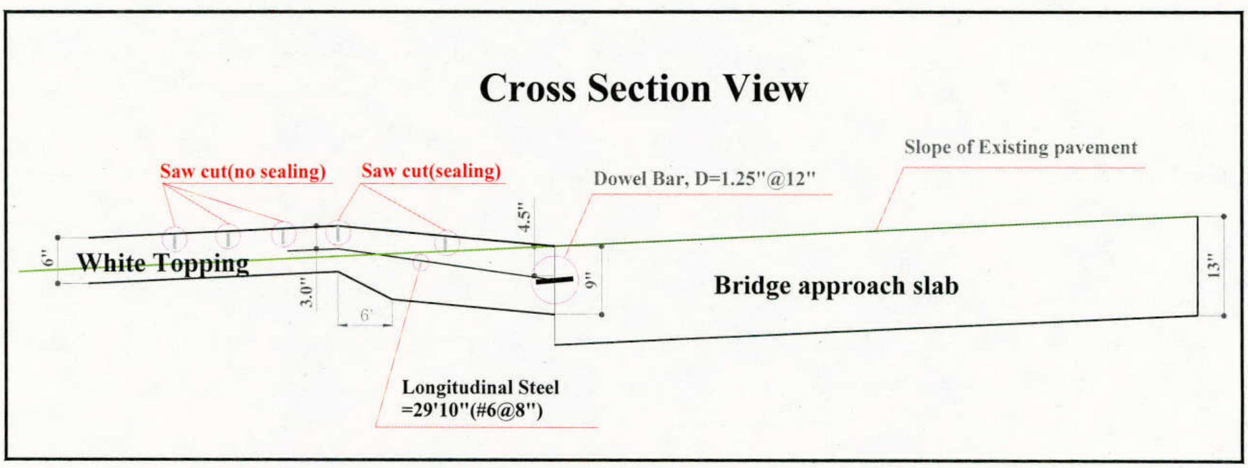

Figure 2.8 Transition Section Design (cross section view)

2.2 Emory Project

The Emory section is located at the intersection between US 69 and SH 19 as indicated in Figure 2.9. Primary distresses in this section were rutting and shoving

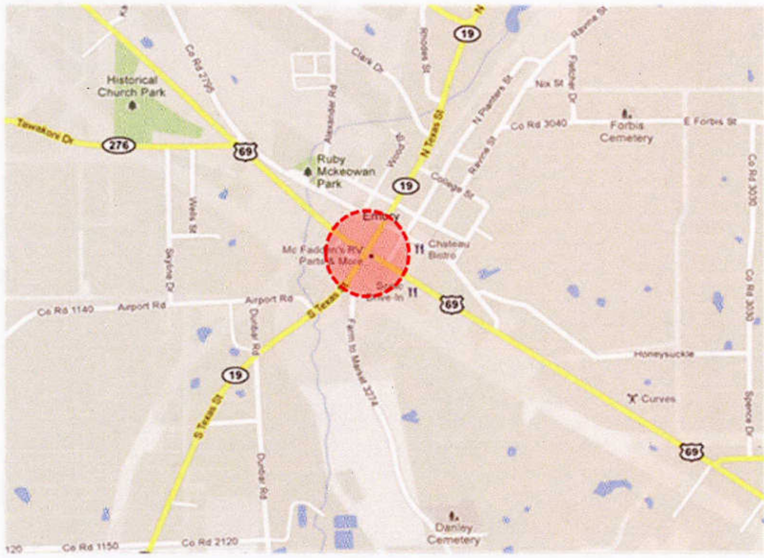

Figure 2.9 Location of the Section

2.2.1. Thickness Design

As discussed earlier, input variables required for the slab thickness design in the mechanistic-empirical whitetopping design include *k*-value, thicknesses of ACP and base, moduli of base and concrete, and ESALs. As illustrated in Figure 2.10, the *k*-value can be back-calculated from the FWD data, and the thicknesses of ACP and base layer can be directly measured by coring samples. The modulus of base can be evaluated by DCP tests. The information on ESALs were obtained from TPP (Transportation Planning and Programming Division) of TxDOT. The *MR* and E_{PCC} were assumed to be 620 psi 4,000,000 psi, respectively. Figure 2.11 indicates the locations where FWD, DCP, and coring were performed by TxDOT personnel. Based on the inputs obtained, design thicknesses were calculated for design lives of 10 and 20 years with various moduli of asphalt concrete.

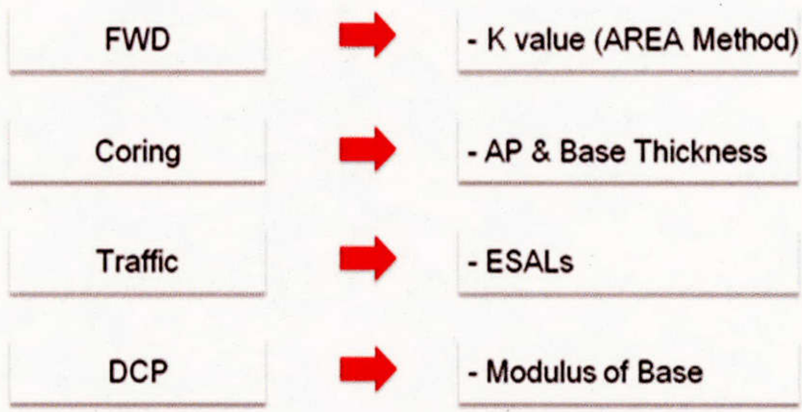

Figure 2.10 Data Collected from Field Testing

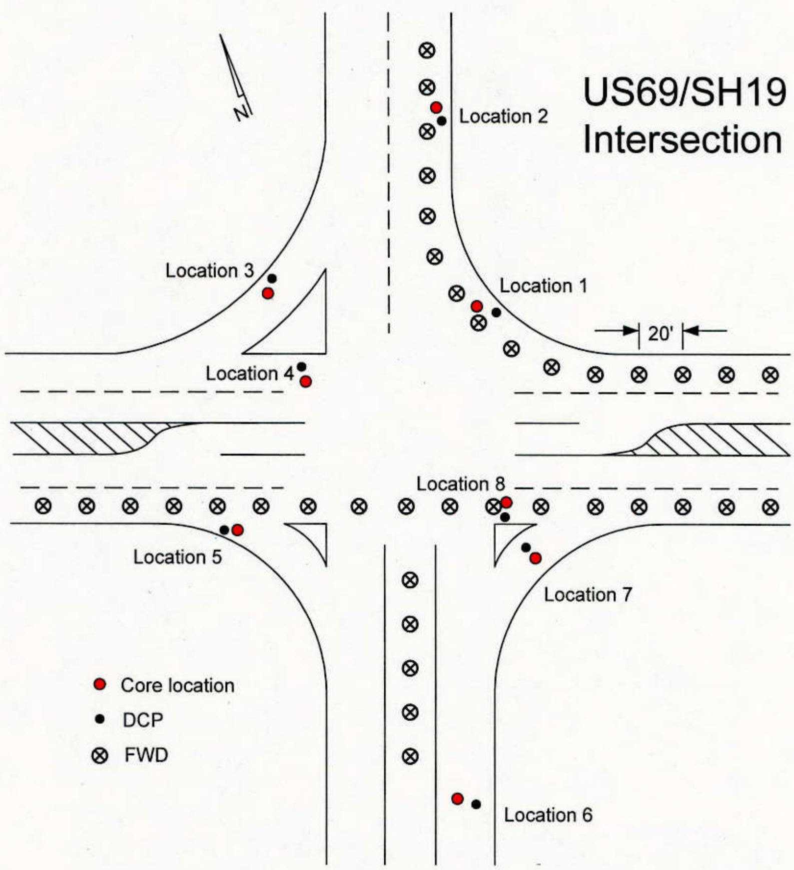

Figure 2.11 Location for Coring, DCP and FWD

2.2.1.1 FWD data

To evaluate the *k*-value, the FWD data obtained from the TxDOT was used. Tables 2.6, 2.7, and 2.8 show the FWD data from different locations. The FWD deflections were normalized to 9000 lbs. Figure 2.12 shows the *k*-values for the cumulative percentage of sections.

Table 2.6 FWD Data of Section (East Bound)

# of Point	Location of sensors (in.) / Deflection (mil)							*k*-value (psi/in)
	0	12	24	36	48	60	72	
1	20.3	12.4	6.2	3.8	2.6	1.8	1.5	290
2	22.4	13.4	6.7	4.1	2.8	2.0	1.7	270
3	23.2	14.1	7.0	4.1	2.7	1.9	1.6	257
4	11.2	7.0	4.5	3.2	2.3	1.6	1.3	430
5	8.1	5.7	3.6	2.6	1.7	1.2	1.0	490
6	6.5	4.7	3.2	2.4	1.8	1.3	1.1	532
7	8.6	5.5	3.5	2.6	1.9	1.4	1.1	539
8	7.2	4.7	3.3	2.6	1.9	1.4	1.2	565
9	8.4	6.2	4.3	3.1	2.2	1.6	1.3	390
10	8.8	5.7	3.9	2.9	2.1	1.5	1.2	486
11	14.7	11.1	6.5	4.1	2.5	1.6	1.3	259
12	27.4	14.8	5.6	2.6	1.5	1.0	0.9	275
13	21.2	13.4	6.2	3.1	1.7	1.1	0.9	282
14	5.6	4.2	2.8	2.1	1.5	1.0	0.8	582
15	4.3	3.3	2.5	2.0	1.6	1.2	1.0	593
16	4.7	3.8	2.9	2.3	1.8	1.3	1.1	458
17	5.5	4.3	3.2	2.5	1.8	1.3	1.1	456
18	5.9	4.3	3.1	2.4	1.8	1.3	1.1	535
19	7.1	5.5	3.8	2.8	1.8	1.2	0.9	409
20	10.9	6.3	3.1	2.1	1.4	1.0	0.8	574
21	7.2	4.9	3.0	2.0	1.5	1.1	0.9	611
22	10.0	5.8	3.4	2.3	1.6	1.1	0.9	571
23	11.1	6.6	3.9	2.6	1.8	1.2	1.0	497
24	16.8	9.0	3.4	2.2	1.5	1.1	0.9	443

Table 2.7 FWD Data of Section (Route Intersection)

# of Point	Location of sensors (in.) / Deflection (mil)							k-value (psi/in)
	0	12	24	36	48	60	72	
1	11.3	7.2	3.4	2.3	1.6	1.2	1.1	500
2	17.6	9.5	3.8	2.2	1.6	1.2	1.1	414
3	6.0	4.3	3.0	2.2	1.6	1.2	0.9	578
4	10.6	7.0	3.4	2.2	1.6	1.2	1.0	507
5	13.8	8.1	4.1	2.6	1.8	1.3	1.1	443
6	13.8	7.7	4.2	2.7	1.9	1.4	1.1	454
7	7.9	5.2	3.5	2.6	1.9	1.3	1.1	537
8	7.9	5.6	3.9	2.9	2.2	1.6	1.3	451
9	9.2	7.4	4.6	2.9	1.8	1.3	1.1	342
10	29.4	14.1	6.4	3.3	2.0	1.4	1.2	267
11	15.4	8.8	4.6	2.6	1.5	0.9	0.8	408
12	39.5	15.6	5.0	2.4	1.5	1.0	0.9	243
13	20.5	10.8	4.7	2.8	1.8	1.2	1.1	354
14	24.2	12.5	5.4	3.0	1.9	1.1	1.3	308
15	22.0	11.3	4.9	2.7	1.8	1.3	1.1	340
16	18.8	9.0	4.1	2.4	1.7	1.3	1.1	414
17	16.1	8.2	3.9	2.4	1.6	1.2	1.0	453
18	12.9	7.6	3.7	2.2	1.5	1.1	1.0	483
19	18.2	8.7	3.5	2.0	1.4	1.0	1.0	442
20	19.6	9.2	3.4	1.8	1.3	1.0	0.8	428
21	19.5	9.6	3.8	2.1	1.4	1.1	0.9	407
22	18.1	8.8	3.6	2.1	1.4	1.1	1.0	438
23	17.4	7.5	3.0	1.8	1.3	1.0	0.9	499
24	17.6	7.6	3.1	1.9	1.3	1.1	0.9	490
25	19.2	9.1	3.5	2.0	1.3	1.0	0.9	428
26	22.3	11.0	4.0	2.0	1.3	1.0	0.9	365

Table 2.8 FWD Data of Section (North Bound)

# of Point	Location of sensors (in.) / Deflection (mil)							k-value (psi/in)
	0	12	24	36	48	60	72	
1	25.6	9.2	4.0	2.6	1.8	1.3	1.2	369
2	18.0	8.4	3.9	2.3	1.4	0.9	0.7	439
3	27.7	14.0	6.6	4.1	2.6	1.6	1.4	264
4	31.3	13.7	5.7	3.6	2.3	1.6	1.4	271
5	21.2	11.3	6.0	3.8	2.5	1.7	1.4	314
6	17.5	9.2	5.1	3.4	2.1	1.4	1.2	377
7	19.1	9.3	4.0	2.4	1.5	1.0	0.8	408
8	18.4	8.5	3.9	2.5	1.6	1.0	0.9	431

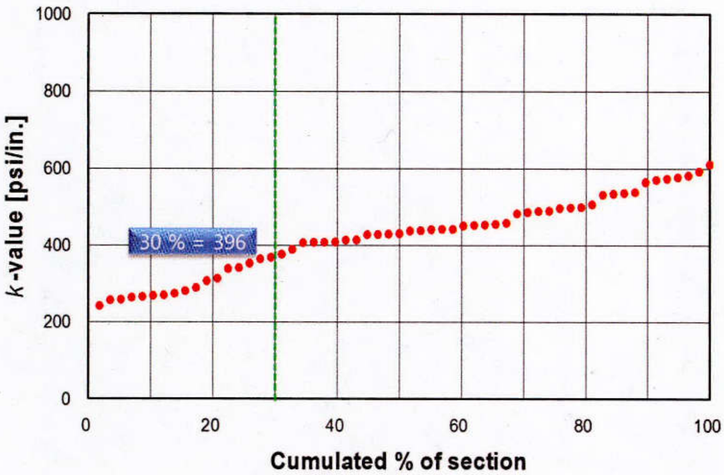

Figure 2.12 *k*-values from FWD

2.2.1.2 Sample Coring

Eight core samples were taken from the section. Figure 2.13 presents the contour of ACP thickness evaluated from the coring samples. The section was divided into eight areas in terms of the ACP thickness. The four main sections shown in Figure 2.13 were considered for whitetopping thickness design.

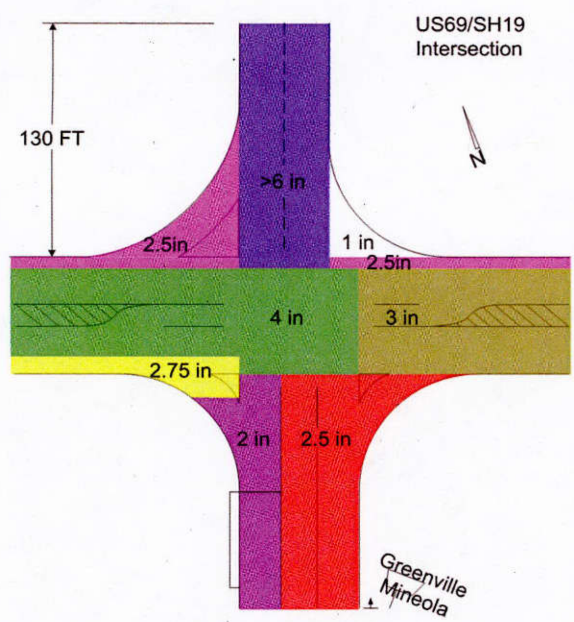

Figure 2.13 ACP Thickness

2.2.1.3 Traffic

The traffic information includes the number of trucks per day for all four directions as shown in Figure 2.14. Based on the traffic data, ESALs were calculated using Eq. 2. Table 2.9 tabulates the traffic information recorded and resulting ESALs computed.

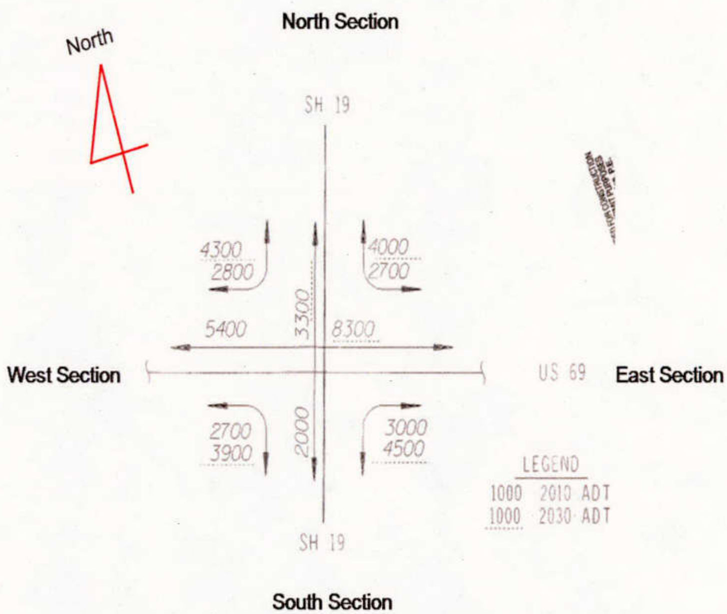

Figure 2.14 Traffic Data and Direction

Table 2.9 Traffic Data and Design ESAL for Each Direction

	Design Year	*Direction 1*	*Direction 2*	*Direction 3*	*Total ADT*	*# Truck (10.7 %)*	*ESALs*
South	2010	2700	2000	3000	7700	824	601,447
	2020				9700	1,038	4,077,342
	2030	3900	3300	4500	11700	1,252	9,092,004
North	2010	2800	2000	2700	7500	803	585,825
	2020				9550	1,022	3,995,327
	2030	4300	3300	4000	11600	1,241	8,951,406
East	2010	2700	5400	3000	11100	1,188	867,021
	2020				13950	1,493	5,869,967
	2030	4000	8300	4500	16800	1,798	13,075,614
West	2010	2800	5400	2700	10900	1,166	851,399
	2020				13700	1,466	5,764,518
	2030	4300	8300	3900	16500	1,766	12,841,284

2.2.1.4 DCP

The relationship between the number of blows and corresponding penetration depths was assessed using DCP test results. Subsequently, CBR values were calculated from Eq. 3 using the slope of DCP plot. The modulus of subbase or subgrade was also estimated by Eq. 4.

Table 2.10 Modulus and CBR Value for Each Section

Location	Unit of material property	Layer 1	Layer 2	Layer 3
Location 1	mm/blow			
	CBR			
	Modulus (ksi)			
Location 2	mm/blow	1.880	17.286	
	CBR	144.02	12.00	
	Modulus (ksi)	61.37	12.51	
Location 3	mm/blow	7.214	20.200	
	CBR	31.93	10.08	
	Modulus (ksi)	23.40	11.19	
Location 4	mm/blow	2.649	8.107	
	CBR	98.06	28.02	
	Modulus (ksi)	47.98	21.52	
Location 5	mm/blow	2.678	12.820	3.651
	CBR	96.90	16.77	68.46
	Modulus (ksi)	47.62	15.50	38.13
Location 6	mm/blow	0.420		
	CBR	771.51		
	Modulus (ksi)	179.66		
Location 7	mm/blow	0.455		
	CBR	705.36		
	Modulus (ksi)	169.64		
Location 8	mm/blow	1.118	4.591	13.980
	CBR	257.68	52.98	15.22
	Modulus (ksi)	89.05	32.36	14.56

2.2.1.5 Thickness Design

Existing ACP thicknesses were measured or estimated from the coring sample and GPR. The base thickness was assumed to be 8 in. Also, it was assumped that MR and E_{PCC} were 650 and 4,000,000 psi, respectively. The k-value was assumed to be 30% of the tested value. Table 2.11 summarizes the input variables used for whitetopping thickness design. Also, Tables 2.12, 2.13, 2.14 and 2.15 show the thickness design evaluated for each of the directions for the design life of 20 years. Because exact values of E_{AC} were not available, the thicknesses were calculated for multiple levels of E_{AC} from 500,000 to 2,000,000 psi. Based on this analysis, a design thickness of 7 in was selected for the project. The saw cut design for Emory whitetopping section is displayed in Figure 2.15. Also, Figure 2.16 illustrates the detailed design for each corner section.

Table 2.11 Input Variables for Whitetopping Thickness

	East		West		South		North	
	10 years	20 years	10 years	20 years	10 years	20 years	10 years	20 years
ESALs ($x10^6$)	4.1	9.1	4.0	9.0	5.9	13.1	5.8	12.8
E_{PCC} (psi)	4,000,000 (assumed)							
t_{BS} (inch)	8.0 (assumed)							
E_{BS} (psi)	50,000 (assumed)							
k (psi/in)	369 (assumed=30% of test result)							
MR (psi)	650 (assumed)							

Table 2.12 Whitetopping Thickness (East Bound – 20 years)

		t_{AC}		
		1 (2" milled)	2 (1" milled)	3
E_{AC}	500,000	21.3	12.9	9.6
	750,000	18.4	11.1	8.3
	1,000,000	16.5	10.0	7.5
	1,250,000	15.3	9.2	6.9
	1,500,000	14.3	8.6	6.5
	1,750,000	13.5	8.2	6.1
	2,000,000	12.9	7.8	5.8

Table 2.13 Whitetopping Thickness (West Bound – 20 years)

		t_{AC}		
		2 (2" milled)	3 (1" milled)	4
E_{AC}	500,000	12.9	9.6	7.8
	750,000	11.1	8.3	6.7
	1,000,000	10.0	7.5	6.1
	1,250,000	9.2	6.9	5.6
	1,500,000	8.6	6.4	5.2
	1,750,000	8.2	6.1	4.9
	2,000,000	7.8	5.8	4.7

Table 2.14 Whitetopping Thickness (South Bound – 20 years)

		t_{AC}		
		0 (2" milled)	1 (1" milled)	2
E_{AC}	500,000	108.3	20.5	12.4
	750,000	93.5	17.7	10.7
	1,000,000	84.3	15.9	9.7
	1,250,000	77.7	14.7	8.9
	1,500,000	72.7	13.8	8.3
	1,750,000	68.8	13.0	7.9
	2,000,000	65.5	12.4	7.5

Table 2.15 Whitetopping Thickness (North Bound – 20 years)

		t_{AC}		
		4 (2" milled)	5 (1" milled)	6
E_{AC}	500,000	7.5	6.4	5.6
	750,000	6.5	5.5	4.8
	1,000,000	5.8	5.0	4.4
	1,250,000	5.4	4.6	4.0
	1,500,000	5.0	4.3	3.8
	1,750,000	4.8	4.1	3.6
	2,000,000	4.5	3.9	3.4

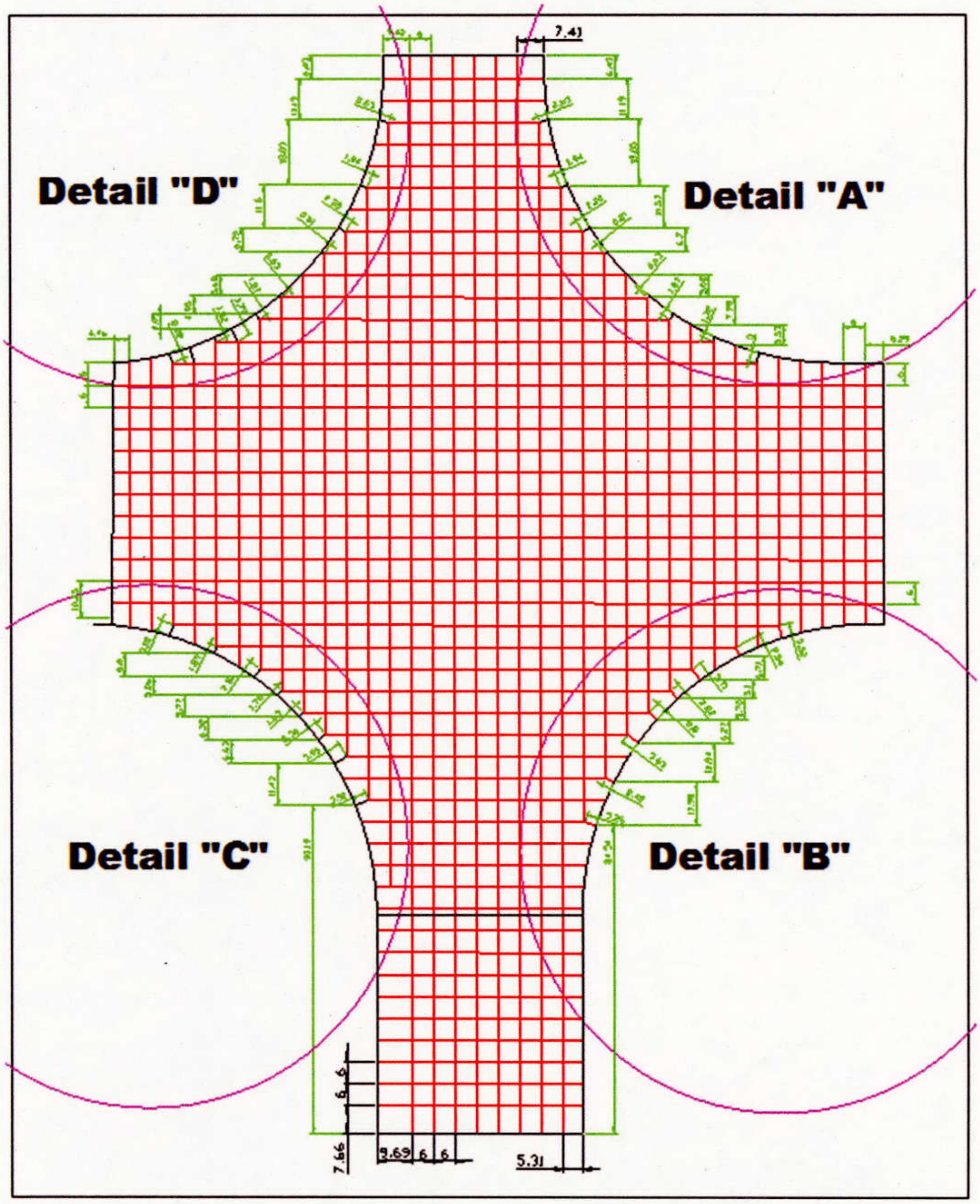

Figure 2.15 Saw Cut Design for Emory Whitetopping Section

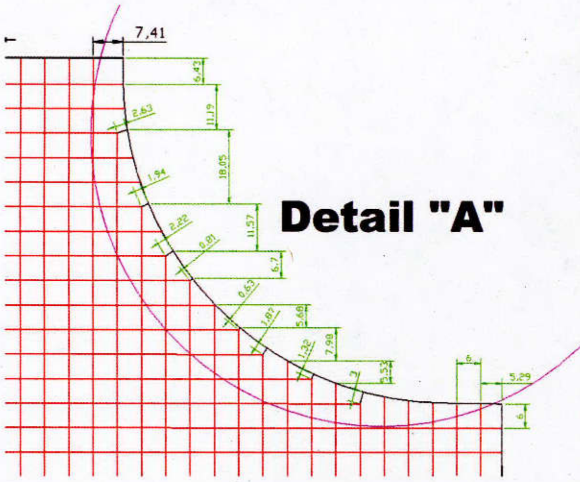

a. Detail "A"

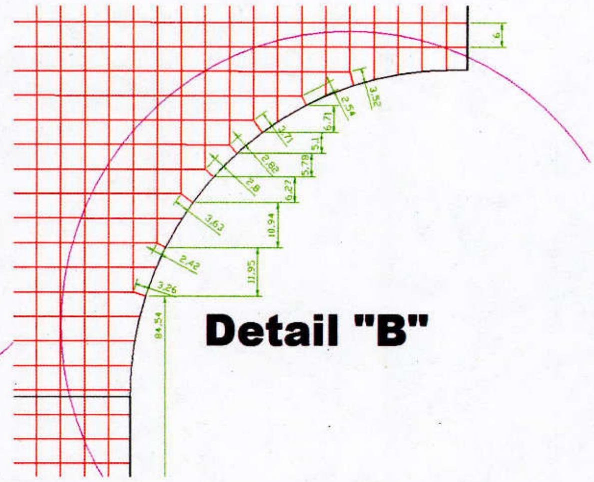

b. Detail "B"

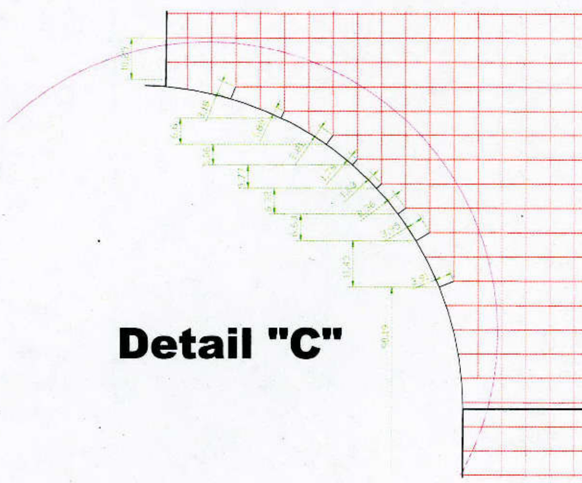

c. Detail "C"

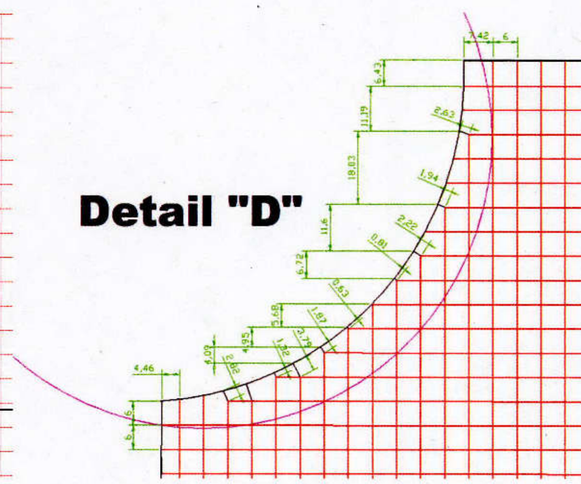

d. Detail "D"

Figure 2.16 Detailed Saw Cut Design for Each Corner

Chapter 3 Behavior Evaluation of Whitetopping

To evaluate the early-age behavior of whitetopping due to environmental and wheel loading, various gages were installed at the whitetopping section at the intersection between US 69 and SH 19 as indicated in Figure 3.1. As discussed earlier, there were a number of rutting and shoving distresses in the existing ACP as shown in Figure 3.2.

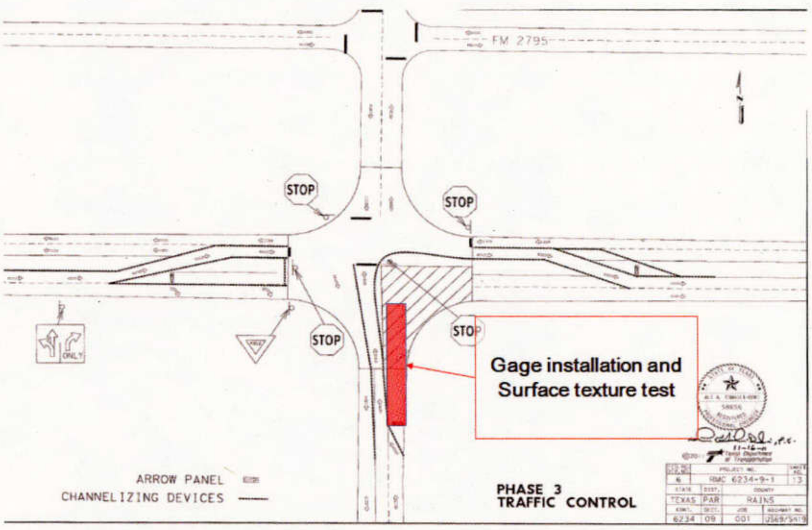

Figure 3.1 Map Showing Location of the Section

Figure 3.2 Distress on Existing Asphalt Pavement

3.1 Gages Installation

3.1.1 Gages Installation Plan

Field testing was conducted to monitor the structural responses of whitetopping sections. As indicated in Figure 3.3 (a), various gages such as vibrating wire strain gages (VWSG), electric resistance concrete strain gages, crackmeters, and thermocouples were employed. The locations of joints and gages are presented in Figure 3.3 (b). The slab size was 6 ft by 6 ft. electric resistance-type concrete strain gages were installed between joints #1 and #2 right on the wheel path to measure the variations of concrete strain due to wheel loading. In addition, VWSGs were installed between joints #2 and #3 and between the wheel paths to monitor the strain variations under environmental loading. Electric resistance-type concrete strain gages were installed at multiple depths in both longitudinal and transverse directions. Additional electric resistance-type concrete strain gages were embedded at the bottom of slab to evaluate the friction with the underlying layer.

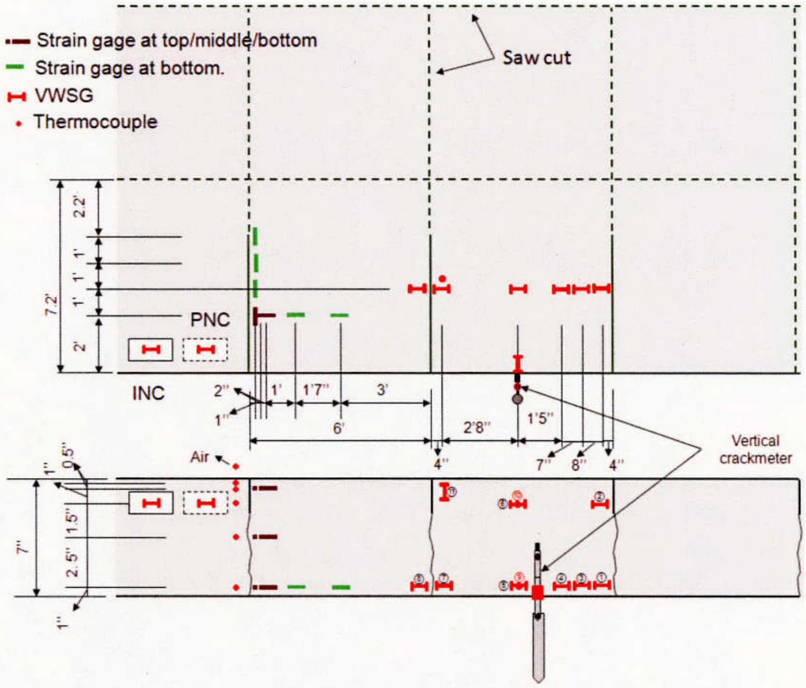

(a) Gage Installation Layout

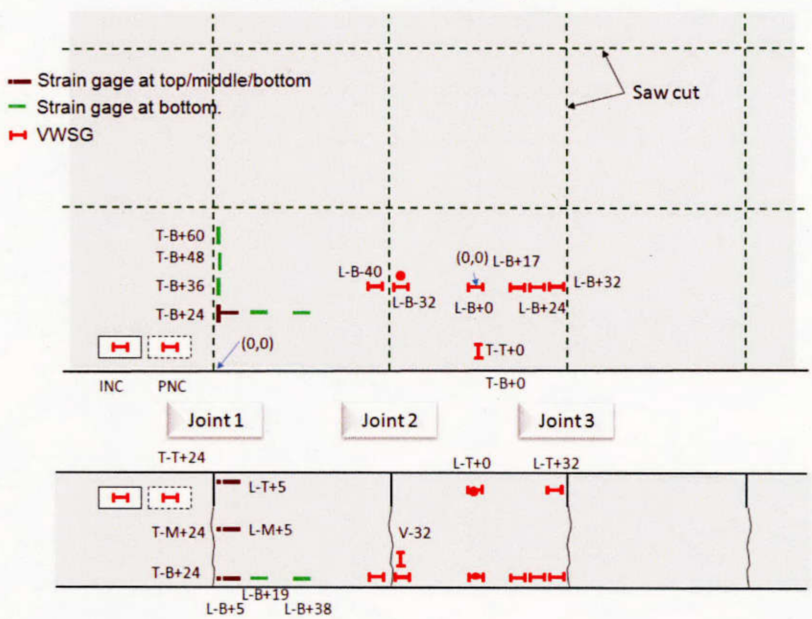

(b) Gages Label and Induced Joints

Figure 3.3 Gage Installation Plans in Emory

3.1.2 Gages Installation in the Field

In order to ensure that the gages are located at the desired positions from adjacent joints, crack inducers (thin steel plate) were installed at joints #1, 2 and 3 as illustrated in Figure 3.4. Figure 3.4 shows that the gages and crack inducers were placed in accordance with the installation plan.

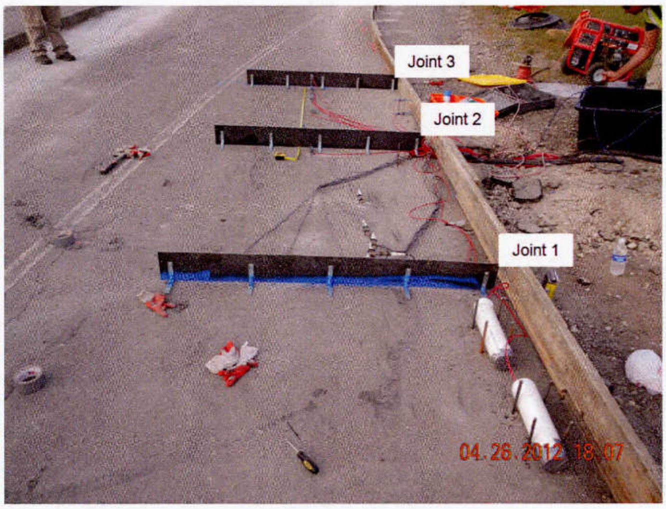

Figure 3.4 Overall Gages Installation at Field

Electric resistance-type concrete strain gages and VWSGs were embedded at different depths in both longitudinal and transverse directions as can be seen in Figure 3.5.

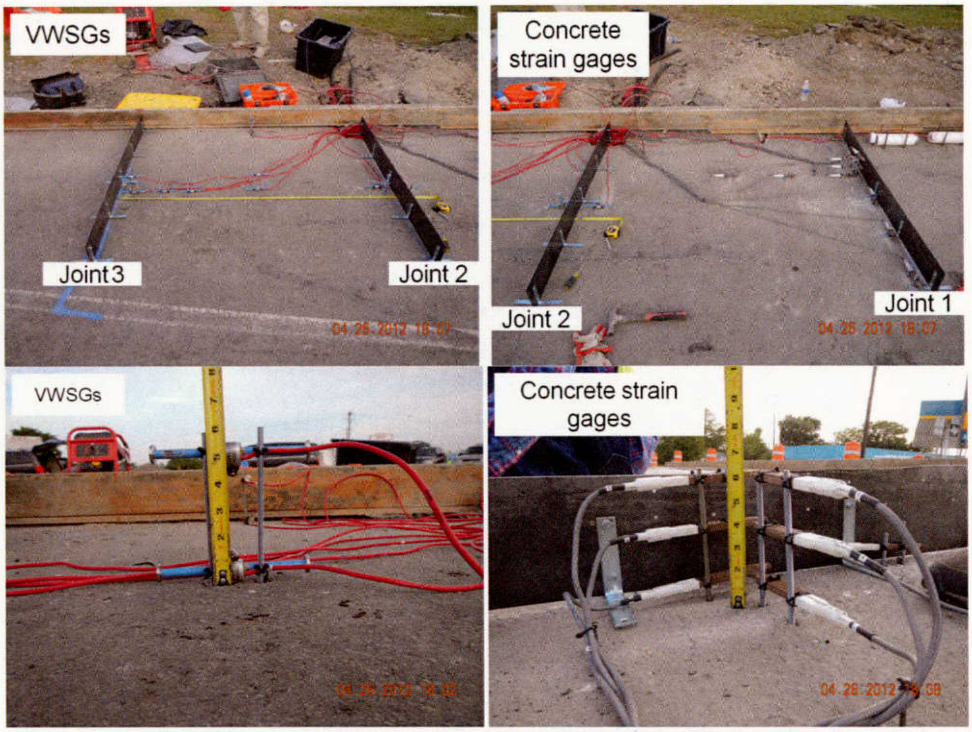

Figure 3.5 Concrete Strain Gages Installation (VWSGs and concrete strain gages)

As shown in Figure 3.6, thermocouples were placed at various positions to measure the nonlinear temperature profile along the slab depth. Porous non-stress cylinder (PNC) and impervious non-stress cylinder (INC) were installed a few inches below the surface of whitetopping slab (Choi and Won 2010). The NC operates in such a way that the concrete filled inside the NCs is fully isolated from the surrounding concrete by means of a smooth-walled plastic (PVC) tube, allowing it to move freely without any influence of external restraint. On the inner surface of the plastic tube, a single layer of porous fabric was attached to reduce the friction at the plastic wall-concrete interface and accommodate the radial volume expansion of the NC specimen. Because the NC specimen has the same properties as the surrounding concrete, the measured strain from the concrete specimen inside the NC purely represents the unrestrained strain of concrete slabs under environmental loadings. Two different types of NCs were employed. One was INC, which does not allow moisture exchange to or from the surrounding concrete. Thus, the strain measured from the concrete inside the INC presents solely thermal strain at the depth of installation. The other was PNC, which was designed to allow moisture exchange with the surrounding concrete through the holes in the tube surface. Accordingly, the strain monitored from the concrete inside the PNC is the sum of drying shrinkage and thermal strain. By subtracting the strain measured by the INC from the strain measured by the PNC, the drying shrinkage strain over time can be estimated. Also, a crackmeter was installed in the vertical direction as soon as concrete was set to measure the vertical relative movement of slab edge due to warping and curling. All the measured data was stored in real time to the data logger.

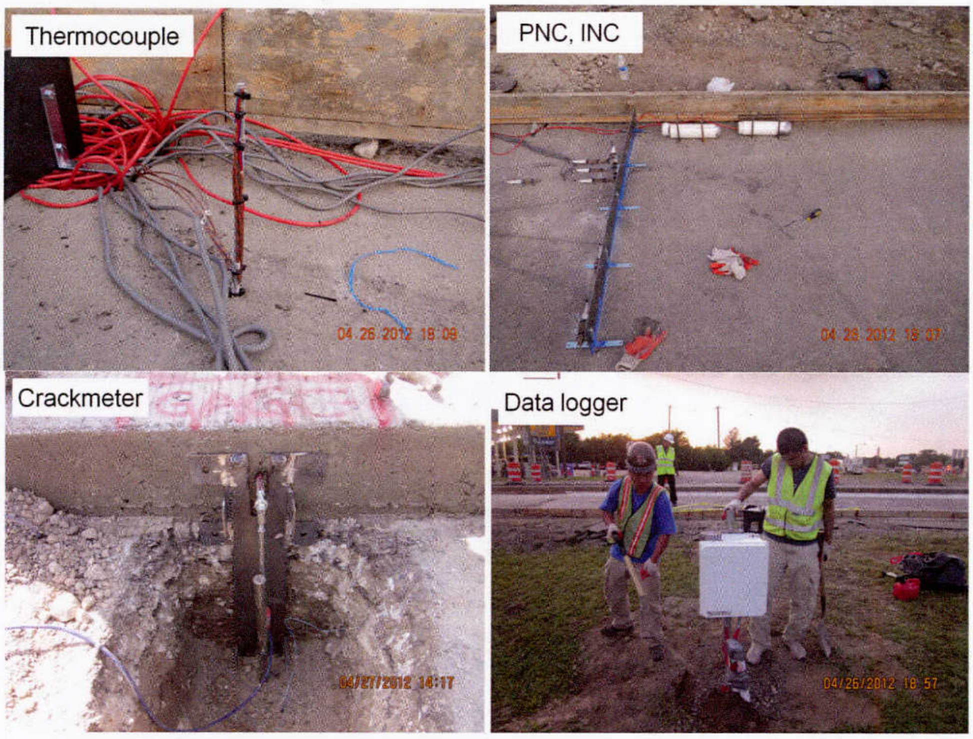

Figure 3.6 Thermocouples, PNC, INC, Crackmeter and Data Logger System

3.2 Whitetopping Construction

To secure a better bond condition between whitetopping and existing asphalt pavement, the surface of existing asphalt concrete pavement was cleaned with a brush before concrete was placed as illustrated in Figure 3.7(a). Only a deck finisher was employed during the concrete placement without a vibrator. As shown in Figure 3.7 (b) and Table 3.1, as soon as the concrete finishing operations were completed, i.e., within an hour after paving initiation, the tinning was commenced. The concrete placement was started and finished at 7:28 and 9:45 AM, respectively. The curing operation started at 10:30 AM. Subsequently, the saw cutting began at 1:30 PM.

(A) Surface Preparation and Concrete Placement

(b) Finishing and saw cut

Figure 3.7 Whitetopping Construction Procedures in Emory

Table 3.1 Construction Sequences

Time	Items
7:25	1st truck arrived
7:28	Start placing concrete from 1st truck + deck finisher
7:45	Finish pouring concrete from 1st truck
7:45	2nd truck arrived
7:49	Start placing concrete from 2nd truck
8:00	Finish pouring concrete from 2nd truck
8:03	3rd truck arrived
8:07	Start placing concrete from 3rd truck
8:17	Finish pouring concrete from 3rd truck
8:31	4th truck arrived
8:33	Tinning
8:37	Start placing concrete from 4th truck
8:50	PNC and INC installation
9:00	Finish pouring concrete from 4th truck
9:30	5th truck arrived
9:35	Start placing concrete from 5th truck
9:45	Finish pouring concrete from 5thtruck
10:30	Start spraying curing compound
13:30	Start saw cutting

3.3. Analysis of Testing Results

3.3.1 Concrete Material Properties

Figure 3.8 indicates that the concrete slump was about 6.5 in. It is also noted in Figure 3.9 that fibers were added to concrete. Figure 3.10 displays the relationship between the concrete's thermal strain and corresponding temperature measured by VWSG inside the INC. The result indicates that the coefficient of thermal expansion (CTE) of concrete, evaluated by the slope of temperature-strain curve, was approximately 6.2 microstrain/°F. Note that the slope of temperature-strain curve, CTE, was not consistent over the measurement period, which might indicate the effect of internal relative humidity in concrete on CTE (Yeon et al. 2009; Yeon et al. 2013).

Figure 3.8 Concrete Slump Test

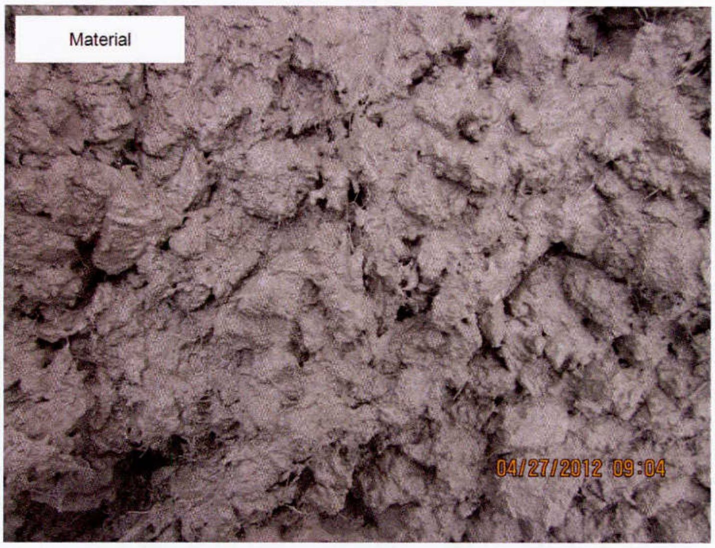

Figure 3.9 Fiber in Concrete

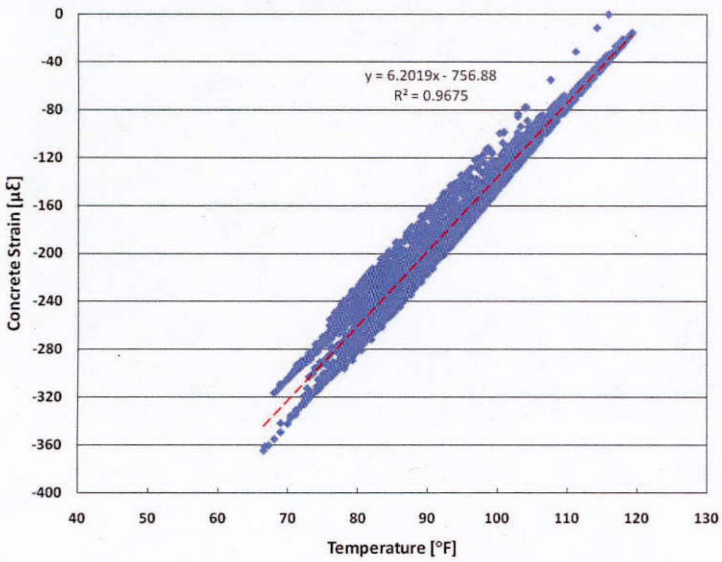

Figure 3.10 Concrete Coefficient of Thermal Expansion (CoTE)

3.3.2 In-Situ Evaluation of Concrete Drying Shrinkage

The drying shrinkage of concrete evaluated from PNC and INC is presented in Figure 3.11. As previously described, the drying shrinkage development can be estimated by subtracting the strain measured by INC from that measured by PNC. It is noted that most of the concrete shrinkage evolved within the first 7 days. Thereafter, the development of drying shrinkage tended to stabilize. The drying shrinkage developed during the first 50 days was about 50 microstrains, which is relatively small.

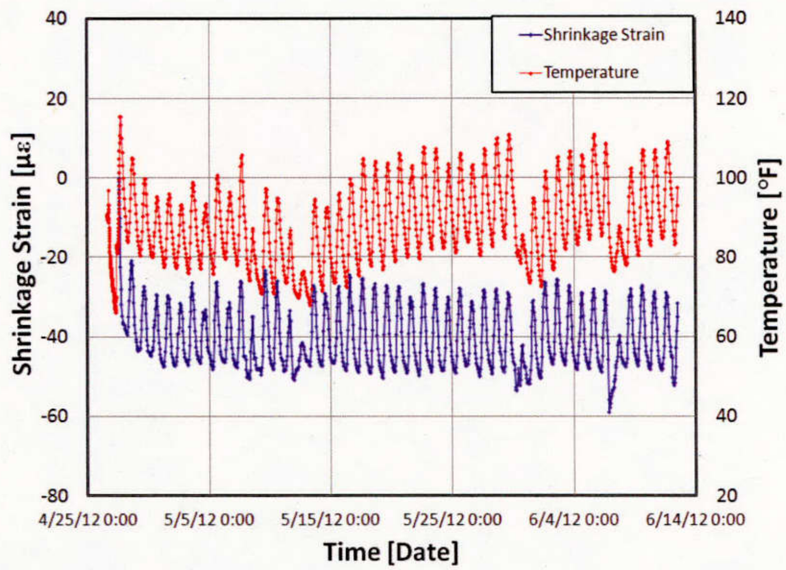

Figure 3.11 Concrete Drying Shrinkage Evaluated from PNC and INC

3.3.3 Concrete Strain from VWSGs

The concrete strains due to temperature and moisture variations at the top and bottom of slab in both longitudinal and transverse directions are illustrated in Figures 3.12 (a), (b), and (c), respectively. The concrete strain variation was the smallest at the center of slab and the largest near the free edge. This is because the magnitude of external restraint is typically much smaller near the free edge than at the interior.

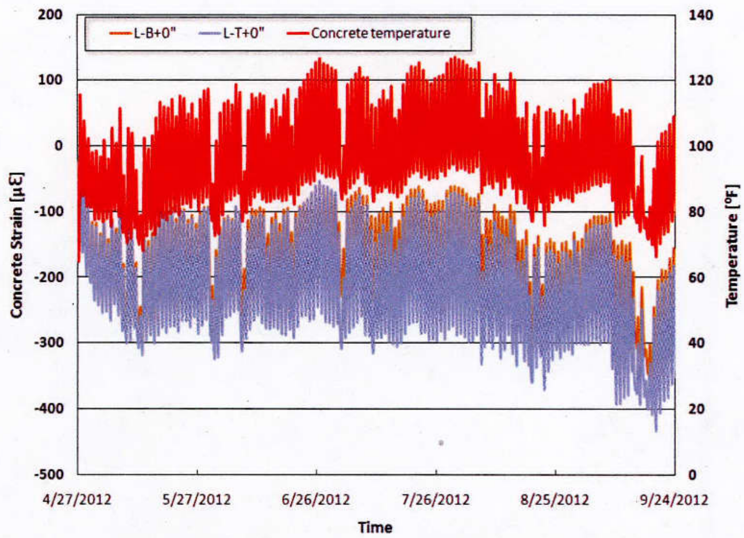

(a) Top and Bottom Concrete Strain in the Longitudinal Direction at the Center of Slab Between Joint #2 and 3

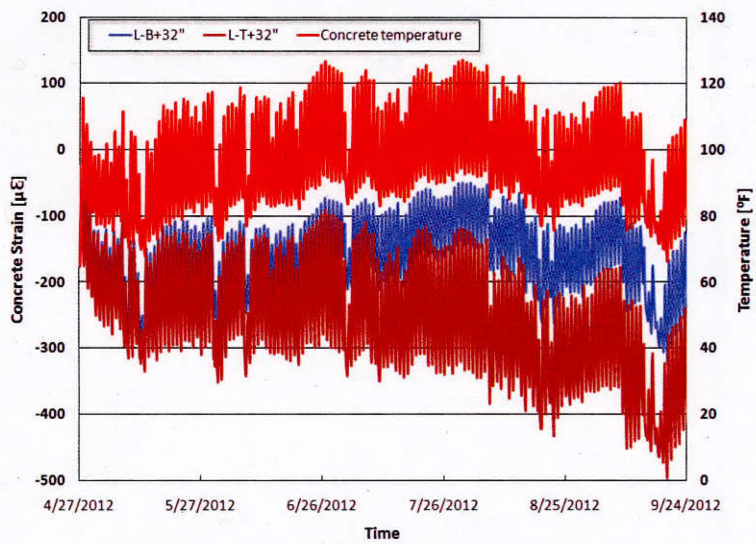

(b) Top and Bottom Concrete Strain in the Longitudinal Direction Near Joint #3

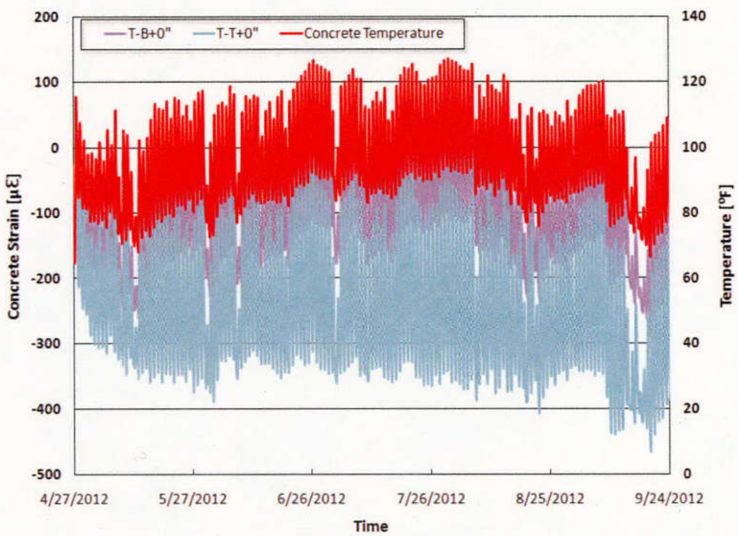

(c) Top and Bottom Concrete Strain in the Transverse Direction Near Free Edge (from VWSGs)

Figure 3.12 Variations of Concrete Strain

3.3.4 Crack Development

The variations of concrete strain at the top, middle, and bottom are presented in Figures 3.13 (a), (b) and (c), respectively. Figures 3.13 (a) and (b) demonstrate that the first crack occurred in the test section during the night time at 6th day when concrete temperature decreased. After the first cracking on May 3, the daily variations of concrete strain significantly increased at the top and middle. The daily concrete strain variations at the bottom, however, were not comparable to those at the middle and top. Also, when cracked, the concrete slab curled up, exhibiting the concrete strain at the top went into compression whereas that at the bottom went into tension. The concrete strain fluctuation at the mid-depth was quite small. This is probably because the position of gage was close to the neutral axis. The concrete strain at the middle moved to compression side when the crack occurred, which indicates the neutral axis was located slightly below the mid-depth due to positive bond with the base layer. Based on the information obtained from the gages, it appears that the crack occurred at Joint #1 location, which is close to the electric strain gages and slightly far from the VWSGs. When a crack occurred on May 3, only two VWSGs close to Joint #1 moved to tension side as shown in Figure 3.13 (c). The concrete gages placed between Joint #1 and #2 did not detect the crack occurrence. Moreover, the rest of the VWSGs 9ft. away from Joint #1 did not capture any concrete strain changes, mostly likely because of good bond condition between the whitetopping slab and existing asphalt pavement. It appears that the good bond condition made the concrete strain due to cracking diminish rapidly, as it moves away from the crack location.

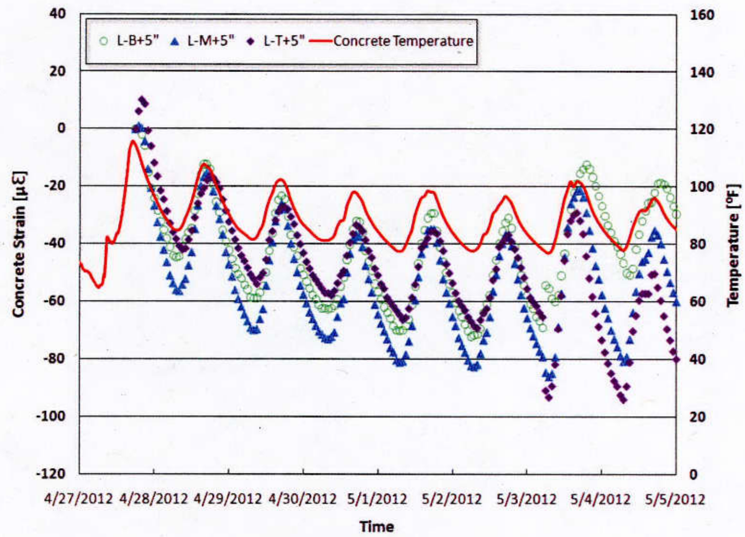

(a) Concrete Strain Variation at Top, Middle, and Bottom in Longitudinal Direction Near Joint #1 (measured by electric strain gages)

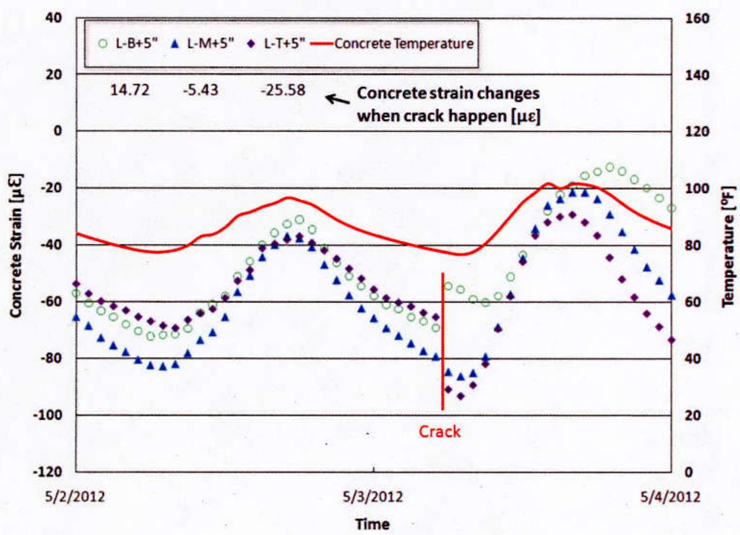

(b) Concrete Strain Changes Near Joint #1 When the 1st Crack was Detected (measured by electric strain gages)

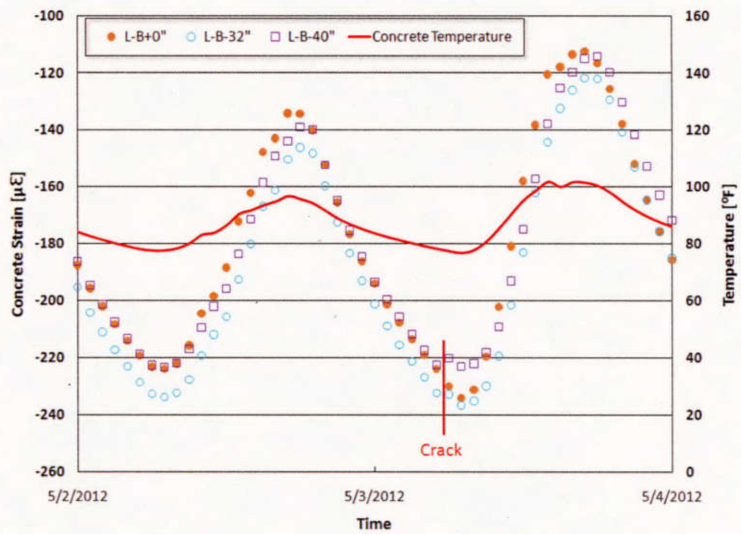

(c) Concrete Strain Changes Near Joint #2 When The 1st Crack Was Detected (measured by VWSGs)

Figure 3.13 Concrete Strain Variations (Before and After Crack)

About 40 days after construction, both electric stain gages and VWSGs detected additional crack occurrence. As shown in Figure 3.14 (a), the behavior of VWSGs near Joint #3 was quite similar to that of electric stain gages near Joint #1 at the time of first cracking; the top concrete element went into compression while the bottom concrete element went into tension. The electric stain gages near Joint #1 also captured the concrete strain changes due to additional cracking as can be seen in Figure 3.14 (b). However, the concrete strain variations were not as significant as those at the first cracking at Joint #1. Figure 3.14 (c) illustrates the variations of concrete strain at the bottom along the longitudinal position when the second crack occurred. When the second crack occurred, the most of bottom concrete elements between Joint #1 and #3 moved to tension side, whereas some bottom concrete elements experienced compression mainly due to temperature drop.

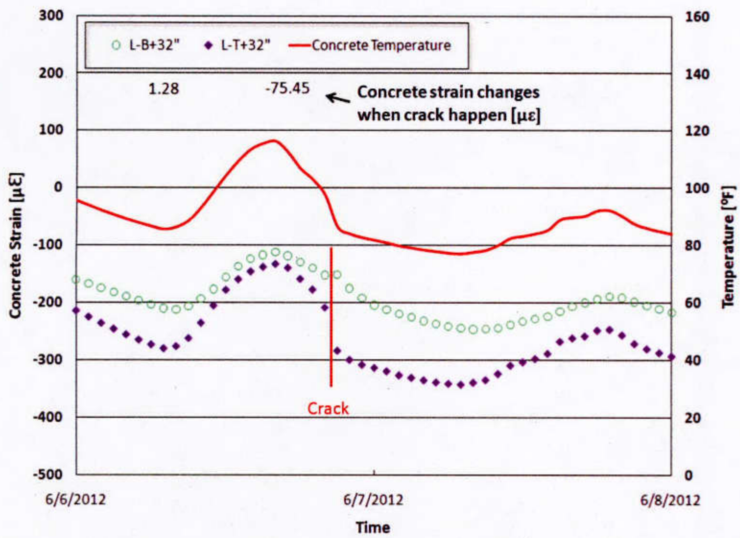

(a) Concrete Strain Changes Near Joint #3 When the Second Crack Was Detected (Measured from VWSGs)

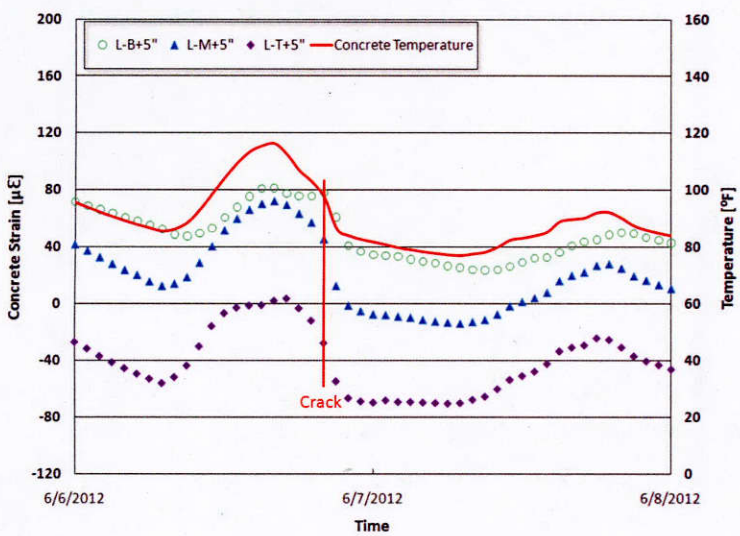

(b) Concrete Strain Changes Near Joint #1 When the Second Crack Was Detected (Measured from Electrical Gages)

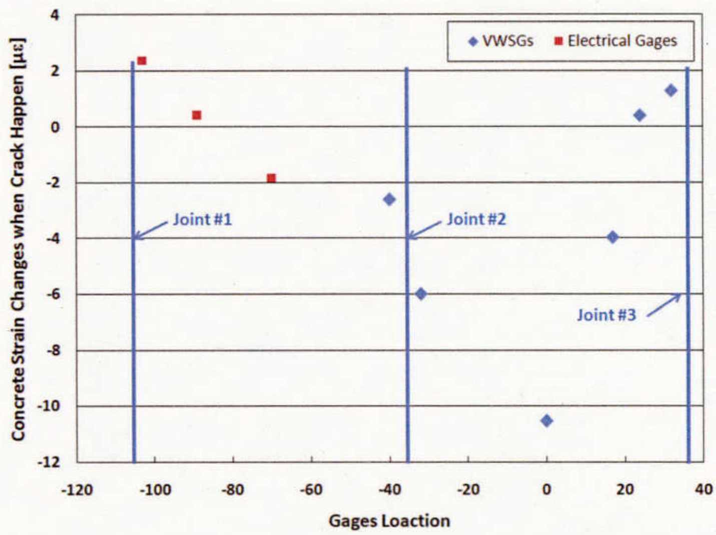

(c) Concrete Strain Changes at Bottom When the Second Crack Was Detected

Figure 3.14 Concrete Strain Changes Related to Joint Pop

Based on the behavior observed in bottom concrete elements at the time of second cracking, it was found that the crack inducer at Joint #2 malfunctioned, and the center of two slab segments between Joint #1 and #3 was located at the mid-slab between two adjacent Joints #2 and #3, as clearly indicated in Figure 3.14 (c). During the 34 days between occurrence of the first and second cracks, the concrete elements close to Joint #1 experienced 34 contraction and expansion cycles due to daily temperature variations, and this may reduce the friction between the concrete slab and existing asphalt pavement near Joint #1. The concrete elements with less friction with asphalt pavement are much easier to move to the tension side when cracking took place. This behavior mechanism resulted in the second crack at the location of Joint #3 on June 6th, 2012.

The condition of cracks at Joints #1, 2 and 3 shown in Figure 3.15 provides information regarding the joint cracking sequence. No crack was found at Joint #2. The crack at Joint #1 was wider than at Joint #3. This finding demonstrates that the crack at Joint #1 took place earlier than that at Joint #3.

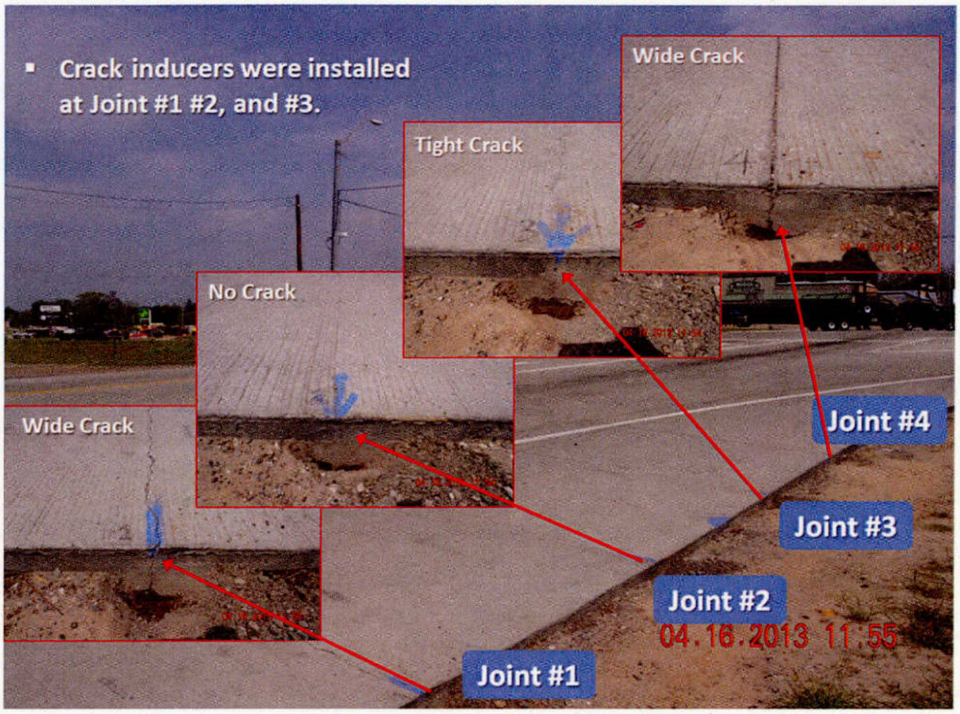

Figure 3.15 Joints Condition

Chapter 4 Development of Whitetopping Design Guidelines

The current TxDOT design procedure for whitetopping is solely based on the number of trucks during design period. It does not account for the existing pavement condition, such as the thickness of asphalt pavement to remain or modulus of asphalt and other layers under the concrete slab. Even though the current whitetopping design procedure has certain merits, such as the simplicity of the design, it does not fully account for the structural condition of the existing pavement. Mechanistic design procedure for whitetopping was developed under TxDOT research project 0-5482, and the procedure was applied to design whitetopping pavements at two locations in this projects. Two whitetopping projects were constructed and their mechanistic behavior and early-age performance have been evaluated, with the primary objective being to validate the design procedure developed in 0-5482. However, the whitetopping projects are less than 2 years old, and the validation of the procedure for long-term performance could not be made. Accordingly, the design guidelines developed also utilized the performance information of a number of whitetopping projects built in Texas over the years, some of which are more than 10 years old.

Two test whitetopping projects were built under this project; one on Loy Lake Drive in Sherman, and the other on US 69 and SH 19 at Emory, both in the Paris District. The Loy Lake Drive project was placed in August, 2011 and the project at Emory was built in April, 2012. Accordingly, as discussed, these two sections were built within the last 2 years and it is too early to draw any conclusions from the early performance of the two sections.

Normally, whitetopping designs involve the following items:

1) slab thickness determinations
2) transition details
3) tie bar, if any
4) sealing joints, if used

Slab thickness determination of whitetopping is not as critical as that for normal paving projects. It is because the size of the whitetopping is small compared with normal highway projects. The project cost differential resulting from using different concrete slab thicknesses is not substantial due to smaller sizes of whitetopping projects. For example, an additional inch of slab thickness would cost $12,000 per lane mile. Accordingly, for a whitetopping project with 6 lanes in both directions with 1,000 ft. long intersection, the additional cost for one inch additional slab thickness would be about $24,000. In addition, at this point, there is no consensus on what the design life should be – 10 years, 20 years, or even longer. At the same time, it is extremely difficult to accurately predict future traffic at intersections. Accordingly, it is recommended that the most conservative slab thickness be used that could be accommodated within the restraints of the existing geometry. The small increase in the construction cost due to the use of conservative thickness designs will be well compensated by better long-term performance of whitetopping. However, the selected slab thickness should be checked against the minimum slab thickness required by the newly developed mechanistic whitetopping design procedure.

The other design element – transition details – is currently dictated by TxDOT Design Standards for whitetopping. The performance of transition areas in all the whitetopping projects in Texas built in accordance with the requirements in TxDOT Design Standards has been performing satisfactorily. It is, therefore, recommended that the current transition details be kept without modifications.

The most difficult design element facing pavement designers during whitetopping design is when asphalt pavement structures become deficient after their removal to provide pavement structures at transition areas. For example, what if all the asphalt pavement structure needs to be removed, leaving flexible base or aggregate base exposed? Is it acceptable to expose flexible base to provide thickened concrete slabs? Or, would it be better if some portions of the asphalt remain in place and concrete slab thickness at transition areas is reduced?

The findings from 0-6274 on the long-term performance of fast-track concrete pavements strongly indicate that replacing asphalt base with increased concrete slab by the same asphalt base thickness provides good performance, as long as traffic consists of passenger vehicles and light trucks, but not a large number of heavy trucks (Ryu et al. 2012). Also, the performance of CRCP sections on US 287 in the Wichita Falls District, where 4-in asphalt base was used, indicate that the use of 4-in asphalt base does not necessarily prevent pumping and other distresses. Figure 4.1 shows severe pumping, where treated soil under the 4-in asphalt base was being pumped out. What if 4-in asphalt was replaced with additional monolithic concrete? The point here is that replacing asphalt base with additional concrete thickness is not necessarily a bad design concept. Figure 4.2 shows continuously reinforced concrete pavement (CRCP) on the frontage road of IH 45 at Sam Houston Tollway in the Houston District, which was placed in 1993. The unique nature of this project is that the concrete was placed directly on top of untreated soil, with no stabilized base between concrete and soil. The slab thickness was increased by 3 inches from the thickness derived for normal pavement structure with a stabilized base. This pavement type is called 'Fast Track Concrete Pavement.' For the last 20 years, the performance has been quite satisfactory, with no single distress in the project. However, it should be noted that the traffic in this project is mostly passenger vehicles and light trucks.

Figure 4.1 Severe Pumping at The Edge of Pavement with Asphalt Stabilized Base

Figure 4.2 Excellent Performance of Fast-Track Concrete Pavement Built In 1993

One of the most common distresses in whitetopping in Texas has been differential slab displacements along longitudinal saw cut joints, as shown in Figures 4.3 and 4.4. In both Figures 4.3 and 4.4, large differential slab displacements at longitudinal joints are noted. The project shown in Figure 4.3 is located on Loop 250 in Midland of the Odessa District. It was placed between April and September of 2001. The Midland project is unique in two aspects; (1) existing asphalt was placed in two lifts, and (2) slab thickness was 3-in and joint spacing was 3-ft by 3-ft, both of the features are not allowed in the current TxDOT whitetopping design procedure. The project shown in Figure 4.4 is on SH 36 at FM 1750 in the Abilene District. In this project, the slab is 4-in thick and the joint spacing is 3-ft by 3-ft. The cause for the slab displacements is not clearly known; however, it appears that different wheel loading condition (one row of slabs under wheel loading while the adjacent row of slabs not under wheel loading) has caused this distress. In normal PCC pavement, tie bars are used to keep lanes together as well as to prevent this type of differential movements. However, it may not be practical to place tie bars in slabs as thin as 3-in. At the same time, it would be feasible to place tie bars if slab thickness is 4-in or larger. Colorado DOT places tie bars at longitudinal joints in their whitetopping. Since 6-ft by 6-ft joint spacing is used in whitetopping in Texas, the differential traffic loading at longitudinal joints is minimized, and the probability of differential slab movements at longitudinal joints is considered minimal.

Figure 4.3 Differential Slab Displacements at Longitudinal Joints in Midland

Figure 4.4 Differential Slab Displacements at Longitudinal Joints in Abilene

Unfortunately, all the whitetopping projects built so far in Texas, except for the afore-mentioned two projects in the Paris District, have 3-ft by 3-ft joint spacing. The performance of the two projects with 6-ft by 6-ft joint spacing needs to be monitored for the differential slab movements potential. Until more conclusive findings are made, it is recommended that tie bars are not used in whitetopping.

Whether joints need to be sealed or not has been a national issue with varying opinions among researchers and practitioners alike. Some states, such as Wisconsin and Minnesota, do not seal the joints in some of their jointed concrete pavement (CPCD). The argument for not sealing joints has been that joint seals are not 100 percent effective in preventing water from getting into joints during rain. On the other hand, joint seals delay the evaporation of water from inside the joints once the rain stops, causing deteriorations of concrete in the joints due to freeze-thaw or other mechanisms. All the whitetopping projects in Texas, except for the section in Loy Lake Drive, did not have joints sealed. No adverse effects of not sealing the joints have been observed in whitetopping projects in Texas; however, all the whitetopping projects, except for the two projects in the Paris District, are located in west Texas, where rainfall is quite small. The performance of the Emory project needs to be monitored for the evaluations of joints with no seals in high rainfall areas. At this point, national efforts are under way by 'Seal or Not Seal (SNS) Group' to positively determine whether sealing is really needed for joints in CPCD or whitetopping. Until conclusive findings and recommendations are suggested by SNS Group, it is recommended that joints in the whitetopping are not sealed.

Chapter 5 Conclusions and Recommendations

The primary objective of this implementation project was to develop whitetopping designs for the two locations in the Paris District and to provide technical support during the PS&E preparation and construction stages.

The design details were provided in terms of the slab thickness, joint details and a transition section design for the success of the whitetopping construction in the two locations mentioned above.

The special design for transition section was developed to minimize the movement caused by different behavior between the approach slab and whitetopping in the Loy Lake Rd project (see the chapter 2.1.3).

The performance of the two projects with 6-ft by 6-ft joint spacing needs to be monitored for the differential slab movements potential to determine whether tie bars are necessary or not. Until more conclusive findings are made, it is recommended that tie bars are not used in whitetopping.

All the whitetopping projects in Texas, except for the section in Loy Lake Drive, did not have joints sealed. No adverse effects of not sealing the joints have been observed in whitetopping projects in Texas. The performance of the Emory project needs to be monitored for the evaluations of joints with no seals in high rainfall areas. At this point, national efforts are under way by 'Seal or Not Seal (SNS) Group' to positively determine whether sealing is really needed for joints in CPCD or whitetopping. Until conclusive findings and recommendations are suggested by SNS Group, it is recommended that joints in the whitetopping are not sealed.

References

Choi, S., and Won, M. C. (2010). "Thermal strain and drying shrinkage of concrete structures in the field." *ACI Materials Journal*, 107(5).

Kim, D., Suliman, M. R., and Won, M. C. (2008). "Literature Review on Concrete Pavement Overlays Over Existing Asphalt Pavement Structures." Center for Transportation Research, The University of Texas at Austin Austin, TX.

Ryu, S. W., Saraf, S., and Won, M. C. (2012). "Project Level Performance Database for Rigid Pavements in Texas, Part II." Texas Department of Transportation, Texas Department of Transportation.

Suh, C., Kim, D., and Won, M. C. (2008). "Development of the Thickness Design for Concrete Pavement Overlays over Existing Asphalt Pavement Structures." Center for Transportation Research, The University of Texas at Austin Austin, TX.

TxDOT (2011). "Pavement Design Guide, Chapter 4 Section 4 Non-Destructive Evaluation of Pavement Structural Properties."http://onlinemanuals.txdot.gov/txdotmanuals/pdm/pdm.pdf.

TxDOT (2011). "Pavement Design Guide, Chapter 8 Section 8 Thin Concrete Pavement Overlay (Thin Whitetopping)." http://onlinemanuals.txdot.gov/txdotmanuals/pdm/pdm.pdf.

Yeon, J. H., Choi, S., and Won, M. C. (2009). "Effect of relative humidity on coefficient of thermal expansion of hardened cement paste and concrete." *Transportation Research Record: Journal of the Transportation Research Board*, 2113(1), 83-91.

Yeon, J. H., Choi, S., and Won, M. C. (2013). "In situ measurement of coefficient of thermal expansion in hardening concrete and its effect on thermal stress development." *Construction and Building Materials*, 38, 306-315.

Appendix A. Whitetopping Design Guidelines

Evaluations of most of the whitetopping projects in Texas revealed that slab thickness has substantial effects on whitetopping performance. From a theoretical standpoint, the findings do make sense, since the stresses in the slab due to wheel loading applications are quite sensitive to slab thickness when slab thickness is within ranges of normal whitetopping (3 to 7 inches). In addition, the major modes of distress in the whitetopping projects in Texas were sliding of concrete slabs and cracking at the joints of transverse and longitudinal saw-cut joints. The sliding of concrete slabs in whitetopping projects invalidates the basic assumptions made in the design of whitetopping, which stipulates that there is full friction between concrete and asphalt. Accordingly, all the whitetopping design procedures developed so far for whitetopping, including the design procedure developed under 0-5482, have intrinsic limitations in their accuracy due to the unrealistic assumption made.

Whitetopping projects are normally applied at intersections, and the surface areas are not extensive. Because of this nature of whitetopping projects, determination of accurate slab thickness is not as critical as in large Portland cement concrete (PCC) pavement projects, since the increase in the cost of a project due to the use of a conservative slab thickness would be minimal. For example, at the current cost of $80 per cubic yard of concrete, the increase in the material cost per inch for a lane mile is about $12,000.

Because of this nature of whitetopping projects, it is strongly recommended that a more conservative slab thickness is used, as long as the geometric conditions allow the selected slab thickness. The selection of the conservative slab thickness could be determined as follows:

1) Evaluate the base/subbase support condition, in terms of modulus of subgrade reaction (k) and modulus values at supporting layers including asphalt layer, at a number of locations in the whitetopping project, using dynamic cone penetrometer (DCP) testing, falling weight deflectometer (FWD) testing, or other methods, such as coring. For the estimation of k value, contact Rigid Pavements and Concrete Materials Branch of CSTMP.
2) Estimate future design traffic in terms of ESALs.
3) The estimated values for the support condition will vary substantially from location to location.
4) Determine the slab thickness using the lower end value from estimated values for support condition and design traffic.
5) Evaluate whether the selected slab thickness can be placed considering geometric conditions of the project site, such as drainage, cross-slope of driveways to adjacent properties, or other constraints. If the answer is no, try to remove the existing pavement

by few inches, and proceed the analysis further until the developed design becomes feasible for the project site.

Another important feature of designs and feasibility analysis of whitetopping is "how much asphalt layer should remain after the removal of asphalt pavement?" General rule of thumb is between 3 and 4 inches. However, there are situations the requirement of a minimum 3 inches of asphalt cannot be met, especially at transition areas. There has been no definite solution to this question. However, long-term evaluations of fast-track concrete pavement projects strongly indicate that the design philosophy of increasing concrete slab thickness instead of providing the same asphalt layer thickness works, as long as traffic consists of mostly passenger vehicles and light trucks. Accordingly, no requirement is needed for the minimum asphalt layer needed to exist under whitetopping, as long as the support condition is accurately evaluated after asphalt removal and required slab thickness is properly determined.

TEXAS TECH UNIVERSITY
Multidisciplinary Research in Transportation

Texas Tech University Lubbock, TX 79409

P. 806.742.3503 F 806.742.4168